

**T.R.  
KASTAMONU UNIVERSITY  
INSTITUTE OF SCIENCE  
DEPARTMENT OF PHYSICS**

**PRODUCTION AND DECAY OF NEW QUARKS THROUGH  
ANOMALOUS INTERACTIONS AT LHC**

**MOUNA MANSUR ALI ABUKRHIS**

**Supervisor Prof . Dr. Ahmet Tolga TAŞÇI  
Jury Member Prof . Dr. Özgür ÖZTÜRK  
Jury Member Assoc. Dr. Ali BOZBEY**

**MASTER OF SCIENCE THESIS  
DEPARTMENT OF PHYSICS  
KASTAMONU – 2018**

## THESIS CONFIRMATION

This thesis, named “**PRODUCTION AND DECAY OF NEW QUARKS THROUGH ANOMALOUS INTERACTIONS AT LHC**” which was prepared by **Mouna Mansour Ali ABUKHRIS**, was defended in front of the following jury members and it was approved by **unanimous vote** as **Master of Science** at Kastamonu University Institute of Science, **Department of Physics**.

Supervisor

Prof . Dr. Ahmet Tolga TAŞCI  
Kastamonu University



Jury Member

Prof . Dr. Özgür ÖZTÜRK  
Kastamonu University



Jury Member

Assoc. Prof. Dr. Ali BOZBEY  
TOBB University of Economics  
and Technology



29/06/2018

Institute Manager

Assoc. Prof. Dr. Mehmet Altan KURNAZ



## COMMITMENT

All information in this thesis have written according to the ethical behavior and academic regulations of Kastamonu university, in addition what does not belong to me in this study was prepared in accordance with the rules of thesis in Kastamonu university, all kind of statements and reports writing that fully referenced to the source of knowledge and commitment.

I hereby declare that all information in this document has been obtained and presented in accordance with academic rules and ethical conduct. I also declare that, as required by these rules and conduct.

Mouna Mansur Ali ABUKHRIS



## ÖZET

Yüksek Lisans Tezi

### YENİ KUARKLARIN LHC'DE ANORMAL ETKİLEŞİMLER İLE ÜRETİM VE BOZUNUMU

Mouna Mansur Ali ABUKHRIS

Kastamonu Üniversitesi

Fen Bilimleri Enstitüsü

Fizik Ana Bilim Dalı

Danışman: Prof. Dr. Ahmet Tolga TAŞÇI

Bu tezde, Büyük Hadron Çarpıştırıcısında (LHC) anormal üretim işlemi  $pp \rightarrow W^+ bV^+ X$  ( $V = g, \gamma, Z$ ) ile ağır  $t'$  kuarkının tek başına olası üretim (elde edilme) potansiyeli analiz edilmektedir.

Kütle merkezi enerjisi 14 TeV olduğunda  $t'$  kuarkının üretim tesir kesiti ve bozunum genişliği hesaplanmaktadır.  $t'$  kuarkının keşif limitleri 300 – 1000 GeV aralığında ve  $\kappa/\Lambda = 0.01 \text{ TeV}^{-1}$ ,  $\kappa/\Lambda = 0.1 \text{ TeV}^{-1}$  ve  $\kappa/\Lambda = 0.5 \text{ TeV}^{-1}$  değerleri için incelenmiştir.

**Anahtar Kelimeler:** Standart model, LHC, anormal etkileşimler.

**2018, 48 sayfa**

**Bilim Kodu: 202**

## ABSTRACT

MSc. Thesis

### PRODUCTION AND DECAY OF NEW QUARKS THROUGH ANOMALOUS INTERACTIONS AT LHC

Mouna Mansur Ali ABUKHRIS

Kastamonu University  
Graduate School of Natural and Applied Sciences  
Department of Physics

Supervisor: Prof. Ahmet Tolga TAŞÇI

In this thesis, the possible discovery potential for single production of heavy  $t'$  quark via anomalous production process  $pp \rightarrow W^+ bV^+ X$  (where,  $V = g, \gamma, Z$ ), at Large Hadron Collider is analyzed.

We calculate the production cross section and decay widths of  $t'$  quark at center of mass energy of 14 TeV. Discovery limits of  $t'$  quark were investigated in the range of 300 – 1000 GeV for  $\kappa/\Lambda = 0.01 \text{ TeV}^{-1}$ ,  $\kappa/\Lambda = 0.1 \text{ TeV}^{-1}$  and  $\kappa/\Lambda = 0.5 \text{ TeV}^{-1}$ .

**Key Words:** Standard model, LHC, Anomalous interactions.

**2018, 48 pages**

**Science Code: 202**

## ACKNOWLEDGEMENTS

First, I would like to thank God for helping me complete this message, despite the difficulties I faced. And my thanks and appreciation to my country Libya, which gave me this opportunity to complete my studies despite the difficult circumstances that pass through.

I am indeed most grateful to my parents, whose continued love, bolsters and guidance have been my source of strength throughout these years. All my gratitude and thanks to my family, especially my husband and my children for the encouragement they gave me to achieve my studies fruitfully.

I express my deep gratitude to my thesis supervisor Prof Dr. Ahmet Tolga TAŞCI for his efforts, sacrifices, advice and continually monitoring this work. I also want to thank my classmates for the support and advice they gave me throughout this training. My esteem regards goes to the department of Institute of Graduate Studies and Research. I am grateful to all my course instructors for the quality of teaching.

Mouna Mansur Ali ABUKHRIS  
Kastamonu, June, 2018

## TABLE OF CONTENTS

|  | Page |
|--|------|
| ÖZET.....  | iv   |
| ABSTRACT.....  | v    |
| ACKNOWLEDGEMENTS.....  | vi   |
| TABLE OF CONTENTS.....   | vii  |
| INDEX OF FIGURES.....  | ix   |
| INDEX OF TABLES.....   | x    |
| SİMGELER VE KISALTMALAR DİZİNİ.....                                    | xii  |
| 1. INTRODUCTION.....   | 1    |
| 1.1. What Constitutes Our Universe?.....                               | 2    |
| 1.2. The Elementary Particle.....                                      | 2    |
| 1.2.1. Elementary Fermions.....  | 3    |
| 1.2.1.1. <i>Quark Elementary Fermions</i> .....                        | 3    |
| 1.2.1.2. <i>Leptons</i> .....  | 4    |
| 1.2.2. Bosons.....   | 5    |
| 1.2.2.1. <i>Higgs boson</i> .....                                      | 6    |
| 1.3. Composite Particle (Hadrons).....                                 | 6    |
| 1.3.1. Baryons.....  | 7    |
| 1.3.2. Mesons.....   | 9    |
| 1.4. The Four Forces in Nature.....                                    | 9    |
| 1.4.1. The electromagnetic force.....                                  | 10   |
| 1.4.2. The strong force.....   | 10   |
| 1.4.3. The gravity force.....  | 11   |
| 1.4.4. The weak force.....   | 11   |
| 1.5. Antiparticle.....   | 12   |
| 1.6. Interactions.....   | 13   |
| 1.6.1. Electroweak interactions.....                                   | 13   |
| 1.7. The Standard Model.....   | 14   |
| 1.8. Beyond the Standard Model.....                                    | 15   |
| 1.9. The Large Hadron Collider.....                                    | 16   |
| 1.9.1. Main detectors in LHC.....                                      | 16   |
| 1.9.1.1. <i>Atlas Detector</i> .....                                   | 16   |
| 1.9.1.2. <i>Detector (CMS)</i> .....                                   | 17   |
| 1.9.1.3. <i>Alice Detector (A Large Ion Collider Experiment)</i> ..... | 18   |
| 1.9.1.4. <i>Beauty Detector: Large Hadron Collider</i> .....           | 19   |
| 1.9.2. How the Large Hadron Collider Works.....                        | 20   |
| 1.9.2.1. <i>Acceleration</i> .....                                     | 20   |
| 1.9.2.2. <i>Collision</i> .....  | 21   |
| 1.9.2.3. <i>Data and results of the Large Hadron Collider</i> .....    | 23   |

|  |    |
|--|----|
| 2. CALCULATIONS .....  | 25 |
| 2.1. Introduction .....  | 25 |
| 2.2. The Anomalous Interactions Through The Heavy Quarks .....   | 26 |
| 2.3. Decay Widths And Branchings .....   | 27 |
| 2.4. The Cross Sections And Analysis Of The Process $pp \rightarrow W^+ bV^+ X$<br>For $t'$ Signal. .... | 32 |
| 3. CONCLUSION .....  | 45 |
| REFERENCES.....  | 46 |
| CV .....   | 48 |





## INDEX OF FIGURES

|  | Page |
|--|------|
| Figure 1.1. Hadronlar .....  | 7    |
| Figure 1.2. Beta dissolution. ....   | 11   |
| Figure 1.3. The standard model of particle physics .....   | 15   |
| Figure 1.4. A Toroidal LHC Apparatus(ATlas) .....  | 17   |
| Figure 1.5. Compact Muon Solenoid (CMS).....   | 18   |
| Figure 1.6. A Large Ion Collider Exprimnt (Alice). ....  | 19   |
| Figure 1.7. Large Hadron Collider Beauty (LHC-B).....  | 20   |
| Figure 1.8. The accelerators in The Large Hadron Collider (LHC).....   | 21   |
| Figure 1.9. The form of collisions within the Large Hadron Collider .....  | 22   |
| Figure 1.10. Computers in the Large Hadron Collider .....  | 23   |
| Figure 1.11. Computing Center - CERN.....  | 24   |
| Figure 2.1. Total decay width of $t'$ depending on its mas .....   | 32   |
| Figure 2.2. Total cross sections for the signal with cuts $P_T=50$ GeV and $ \eta_{j,\gamma}  < -2.5$ at the center of mass energy $\sqrt{S} = 14$ TeV for PI, PII and PIII. ....      | 42   |
| Figure 2.3. Total cross sections for the backgrounds with cuts $P_T=50$ GeV and $ \eta_{j,\gamma}  < -2.5$ at the center of mass energy $\sqrt{S} = 14$ TeV for PI, PII and PIII ..... | 42   |

## INDEX OF TABLES

|  | <b>Page</b> |
|--|-------------|
| Table 1.1. Properties of the QUARKS.....   | 4           |
| Table 1.2. Leptons.....  | 5           |
| Table 1.3. The baryons with some characteristics. ....   | 8           |
| Table 1.4. The mesons .....  | 9           |
| Table 1.5. Particle and antiparticle.....  | 12          |
| Table 2.1. Branching rates (%) and decay widths of the heavy t quark for PI ...  | 28          |
| Table 2.2. Branching rates (%) and decay widths of the heavy t quark for PII..   | 30          |
| Table 2.3. Branching rates (%) and decay widths of the heavy t quark for PII .   | 31          |
| Table 2.4. Total cross sections for t' signal at the center of mass energy<br>$\sqrt{S}=14$ TeV .....  | 33          |
| Table 2.5. Total cross sections for the backgrounds at the center of mass<br>energy of $\sqrt{S}=14$ TeV .....   | 34          |
| Table 2.6. The cross sections (in pb) for t' signal at the process $pp \rightarrow \gamma b$ with<br>$ \eta_{j,\gamma}  < -2.5$ and $P_T = 50$ GeV at the center of mass energy $\sqrt{S} = 14$<br>TeV for parametrization PI .....                            | 35          |
| Table 2.7. The cross sections (in pb) for t' signal at the process $pp \rightarrow \gamma b$ with<br>$ \eta_{j,\gamma}  < -2.5$ and $P_T = 50$ GeV at the center of mass energy $\sqrt{S} = 14$<br>TeV for parametrization PII .....                           | 35          |
| Table 2.8. The cross sections (in pb) for t' signal at the process $pp \rightarrow \gamma b$ with<br>$ \eta_{j,\gamma}  < -2.5$ and $P_T = 50$ GeV at the center of mass energy $\sqrt{S} = 14$<br>TeV for parametrization PIII .....                          | 36          |
| Table 2.9. The cross sections for t' signal at the process $pp \rightarrow gb$ with<br>$P_T = 50$ GeV and cuts $ \eta_{j,\gamma}  < -2.5$ at the center of mass energy 14<br>TeV for parametrization PI.....   | 37          |
| Table 2.10. The cross sections for t' signal at the process $pp \rightarrow gb$ with<br>$P_T = 50$ GeV and cuts $ \eta_{j,\gamma}  < -2.5$ at the center of mass energy<br>14 TeV for parametrization PII .....  | 37          |
| Table 2.11. The cross sections for t' signal at the process $pp \rightarrow gb$ with<br>$P_T = 50$ GeV and cuts $ \eta_{j,\gamma}  < -2.5$ at the center of mass energy<br>14 TeV for parametrization PI.....  | 38          |
| Table 2.12. The cross sections for t' The cross sections for t' signal at the<br>process $pp \rightarrow Zb$ with $P_T = 50$ GeV and cuts $ \eta_{j,\gamma}  < -2.5$ at the<br>center of mass energy 14 TeV for parametrization PI.....                        | 38          |
| Table 2.13. The cross sections for t' The cross sections for t' signal at the<br>process $pp \rightarrow Zb$ with $P_T = 50$ GeV and cuts $ \eta_{j,\gamma}  < -2.5$ at the<br>center of mass energy 14 TeV for parametrization PII .....                      | 39          |
| Table 2.14. The cross sections for t' The cross sections for t' signal at the<br>process $pp \rightarrow Zb$ with $P_T = 50$ GeV and cuts $ \eta_{j,\gamma}  < -2.5$ at the<br>center of mass energy 14 TeV for parametrization PIII .....                     | 39          |
| Table 2.15. The cross sections for the backgrounds to the process ( $pp \rightarrow \gamma b$ ),<br>( $pp \rightarrow gb$ ), ( $pp \rightarrow Zb$ ) with cuts $P_T=50$ GeV and $ \eta_{j,\gamma}  < -2.5$ at<br>the center of mass energy 14 TeV for PI ..... | 40          |

|   |    |
|---|----|
| Table 2.16. The cross sections for the backgrounds to the process ( $pp \rightarrow \gamma b$ ),<br>( $pp \rightarrow gb$ ), ( $pp \rightarrow Zb$ ) with cuts $P_T=50$ GeV and $ \eta_{j,\gamma}  < 2.5$ at<br>the center of mass energy 14 TeV for PII.....   | 40 |
| Table 2.17. The cross sections for the backgrounds to the process ( $pp \rightarrow \gamma b$ ),<br>( $pp \rightarrow gb$ ), ( $pp \rightarrow Zb$ ) with cuts $P_T=50$ GeV and $ \eta_{j,\gamma}  < 2.5$ at<br>the center of mass energy 14 TeV for PIII ..... | 41 |
| Table 2.18. The statistical significances values for backgrounds and signal<br>cross sections of $t'$ for PI, PII and PIII) .....   | 43 |



## SYMBOLS AND ABBREVIATION

|                   |                                    |
|-------------------|------------------------------------|
| $\sqrt{s}$        | Center Of Mass Energy              |
| ALICE             | A Large Ion Collider Expropriation |
| ATLAS             | A Toroidal LHC Apparatus           |
| CMS               | Compact Moun Solenoid              |
| LHC               | Large Hadron Collider              |
| LHC-B             | Large Hadron Collider Beauty       |
| $\eta_{j,\gamma}$ | Pseudorapidity                     |
| PS                | Proton Synchrotron                 |
| $P_T$             | Transverse Momentum                |
| QCD               | Quantum Chromo Dynamic             |
| SM                | Standard Model of particle physics |
| SPS               | Super Proton Synchrotron           |
| TPC               | Time Projection Chamber            |

## 1. Introduction

To begin with, the standard model of particle physics (SM) had been developed after a large number of theoretical research and practical research made to describe all that exists in the universe and interactions between particles. This model contributed to the advance of the basic theory of molecules and it aims to illustrate us from where particle physics reached and what had been predicted as the new phenomena afterwards .

Buna Moreover, the standard model has aimed to present a brief idea in terms of what is known as strong and weak interactions with electromagnetic force except gravity including the vital information that must be known. According to the feedback of certain studies, electroweak interaction had been named once after weak interaction was combined with electromagnetic. It is vital to be acknowledged that this specific interaction is one of the most important interactions in particle physics.

Electromagnetic force had been discovered after a period of time when electromagnetic wave radiation had been discovered by Hertz 1885 in the beginning of quantum mechanics. It is also important to note that the electron was the first primary particle to be discovered, weighing about  $\frac{1}{2}$  MeV. Following this, then discovered an unstable particle called the muon, and weighed 100 MeV in cosmic rays. In the past 50 years have yielded results and information that contributed to the standard model, which will lead to a wide range of discussion and questions.

This theory was developed in the early seventies, as one of the theories of quantum field had been compatible with the theory of special relativity and quantum mechanics, where all experiments confirm the validity of the predictions of this theory. However, the main drawback of this theory lies in its non-characterization of the fourth fundamental force; the force of gravity and all the efforts of theoretical physics now focus on the formation of a complete theory, that is, it describes the four basic forces, including the force of gravity. the process of collecting general relativity that deals with gravity with quantum mechanics is one of the most important dilemmas facing modern physics.

## 1.1. What Constitutes Our Universe?

The question that always comes to our mind is what are the components of the world around us and what is its basic structure? It was common that the material consisted of four elements as water, fire, air and dust respectively. However, with time and constant experiments to answer precisely this question, which was its atomic theory. It has been confirmed that the material has only been a group of small particles that could not be divided according to beliefs at the time.

John Dalton announced this theory in the 19th Century and the experiments of Redford and Schidwick have been credited with discovering the nucleus and its particles of protons and neutrons. It should be noted that physicists Schrodinger and Heisenberg should not be forgotten with regard to their development on atomic theory in its final form and now which is known as the Yukawa theory. This theory has been the cornerstone of physics particles 1930 where this theory illustrated the force that made protons and neutrons interconnected within the nucleus. Between the years 1970 and 1960, there had been a great evolution in particle physics. Scientists built particle accelerators through which new particles with a very short lifespan were observed. Noone knew what these particles were or whether they were elementary particles or something unnamed.

It had been a confusing discovery for the scientists the idea that protons and neutrons were not elementary particles as they thought and these other particles were smaller than neutrons and protons were the primary particles that helped shape a new mathematical model. Not only that but also, scientists had recognized that the atomic particles were divided into three elementary particles, which they gave the name of the quarks.

## **1.2. The Elementary Particle**

For centuries, scientist only knew the periodic table which was thought to be at the time that hydrogen was the least mass of all periodic cyclic elements until particles had been discovered a thousand times less than the hydrogen atom. Therefore, this made scientists look into a scientific explanation of this result, which has been resulted in the discovery of the electron. This was considered as the gateway to further research and experiments that resulted in the discovery of protons and neutrons within the nucleus of the atom revolving electrons in closed orbits. However, at the beginning of the 1930s scientists aimed to explain several phenomena for a model's inability to form essentially consisting of protons, neutrons and electrons. Later, they reached a particle accelerator to find an explanation for what was happening around us. At the end of the 1960s, the scientists came up with a striking conclusion that protons and neutrons are primary particles linked by a powerful force called quarks, which are difficult to divide into smaller ones .

### **1.2.1. Elementary Fermions:**

Quarks and leptons are called Fermions. As lepton enters electroweak interactions while quarks enter the strong interactions and electroweak interactions. It is important to note that the leptons without quarks have no standard model at all. These will be mentioned and defined in the study below.

#### **1.2.1.1. Quark *Elementary Fermions*:**

The quark can be called one of the primary particles and the inability of the scientists in order to make the quarks alone to be studied made them take the dispersion experiments in the accelerators of the particles and that led to the knowledge of the existence of three types of quarks. As a result, they discovered that the proton consists of two up quark and one down quark. The Nitron consists of two down quarks and one up quark.

Quark 10<sup>-19</sup> cm, and scientists found that the quark is indistinguishable, that is, the smallest thing in the material and that it is small may not have a size and this conclusion has a negative impact on the mathematical equations used.

There are quarks, anti-quarks and when there are two quarks in a vacuum they must carry a charge opposite each other and turn in the opposite way because once that happens they will clash and then they will disappear .

Moreover, it is the strong force that makes the quarks coherent together in the neutron or the proton. The following table shows the types of quarks with their properties:

Table 1.1. *Properties of the QUARKS.*

| Quark | Mass (GeV/ c <sup>2</sup> ) | Q    | B   | Y    | I <sub>3</sub> | I   |
|-------|-----------------------------|------|-----|------|----------------|-----|
| d     | ≈0.35                       | -1/3 | 1/3 | 1/3  | -1/2           | 1/2 |
| u     | ≈0.35                       | 2/3  | 1/3 | 1/3  | 1/2            | 1/2 |
| s     | ≈0.5                        | -1/3 | 1/3 | -2/3 | 0              | 0   |
| c     | ≈1.5                        | 2/3  | 1/3 | 4/3  | 0              | 0   |
| b     | ≈4.5                        | -1/3 | 1/3 | -2/3 | 0              | 0   |
| t     | ≈173                        | 2/3  | 1/3 | 4/3  | 0              | 0   |

### 1.2.1.2. Leptons

First, lepton is one of the primary particles. It was first named in 1948. It can be said that strong interactions cannot affect this particle and moreover Lepton spins (1/2). There are two types of leptons. The first type of Lepton is thought to include a charge with the most famous leptons. Furthermore, it is assumed as the most interactive and results of the formation of composite particles. Whereas, the second type known as neutrino is less interactive and therefore unable to see much. To note that, Leptons also have six flavours, as shown in the table these are (3.2): electron, electron neutrino (the lightest and most common), muon, muon neutrino, Tau and Tau neutrinos respectively



Leptons have properties such as electric charge, mass and spin. In contrast to quarks, leptons do not affect strong force, while gravity, weak force, and electromagnetic force influence them. As in quarks, each type of lepton has antileptons and has the same properties as the lepton except the charge signal .

Table 1.2. *Leptons.*

| Name              | Symbol         | Antiparticle    | Charge e | Mass (GeV/ c <sup>2</sup> ) |
|-------------------|----------------|-----------------|----------|-----------------------------|
| Electron          | e <sup>-</sup> | e <sup>+</sup>  | -1       | 0.511                       |
| Electron neutrino | $\nu_e$        | $\bar{\nu}_e$   | 0        | Small, but non- zero        |
| Muon              | $\mu^-$        | $\mu^+$         | -1       | 105.7                       |
| Muon neutrino     | $\nu_\mu$      | $\bar{\nu}_\mu$ | 0        | <0.170                      |
| Tau               | $\pi^-$        | $\pi^+$         | -1       | 1.777                       |
| Tau neutrino      | $\nu_\pi$      | $\bar{\nu}_\pi$ | 0        | <15.5                       |

### 1.2.2. Bosons

The bosons are only primary particles carrying the basic forces such as Photon, Gluon, Graviton and Higgs boson respectively.

Different types of bosons and forces will be mentioned and discussed in details later on in this specific study

### **1.2.2.1. Higgs boson**

Since 1964, Peter Higgs has predicted that there has been an initial particle larger than the proton assumed as 200 times when the boson has later been called the Higgs boson. Peter has believed that boson was related to the mass acquisition of particles. However, Higgs boson proved to be practically in Cern by the Large Hadron Collider. The installation and subsequent use of the device will later on be explained briefly in the paper.

It was detected on Wednesday, July 4, 2012, and the required boson was 99.999%. After this particular discovery, the standard model that predicted the existence of this boson has long been validated .

### **1.3. Composite Particle (Hadrons)**

To begin with, the Hadrons are complex particles where they arise from quarks union with each other. When two quarks merge, they become mesons while three quarks form baryons. The following figure can give us a simple idea of what the Hadrons are:

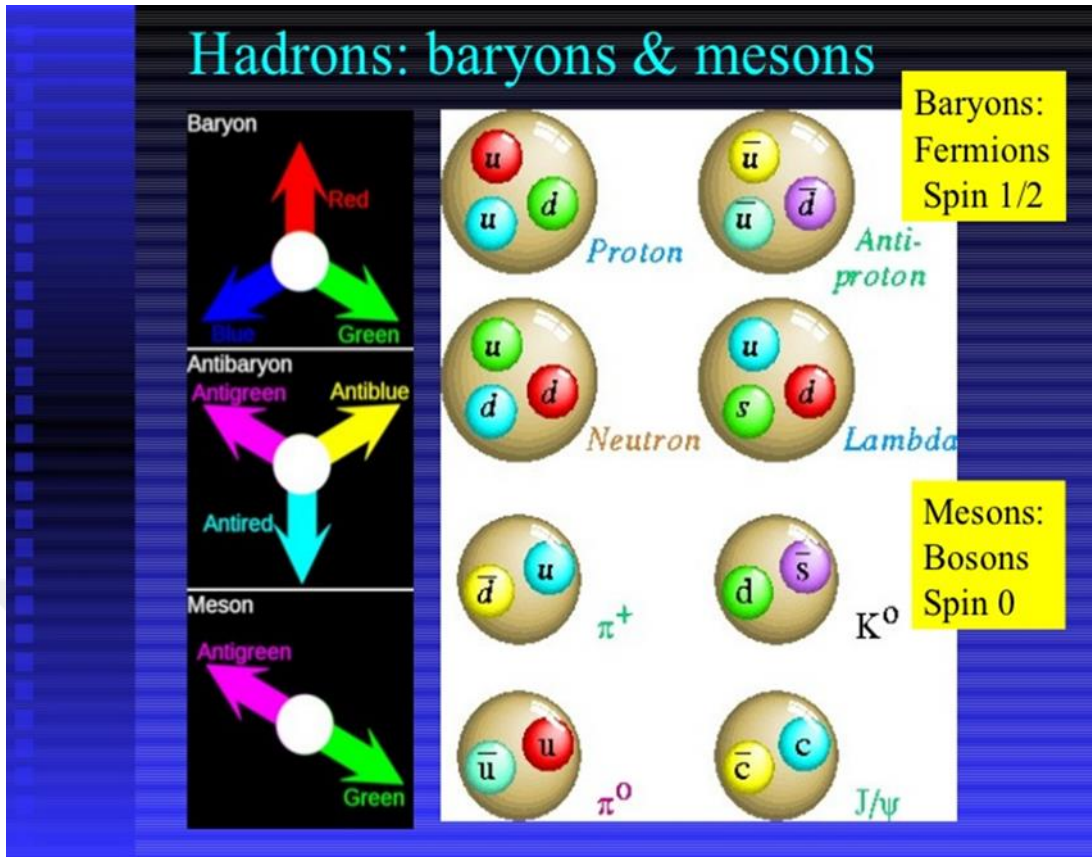


Figure 1.1. Hadronlar.

### 1.3.1 Baryons

Baryons are larger particles than protons. In addition, the baryons possess a half-spinning ( $1/2, 3/2, 5/2, \dots$ ). Baryons are composed of 3 quarks. Protons and neutrons are the best examples of baryons. The following table shows some baryons with some characteristics:

Table 1.3. *The baryons with some characteristics.*

| Particle and symbol            | Charge / proton charge | Antiparticle and symbol   | Charge / proton charge | Rest energy/Mev | Interaction                                   |
|--------------------------------|------------------------|---|------------------------|-----------------|---|
| Proton p                       | +1                     | Antiproton $\bar{p}$  | -1                     | 938             | Strong, weak, electromagnetic                 |
| Neutron n                      | 0                      | Antineutron $\bar{n}$   | 0                      | 939             | Strong, weak                                  |
| Electron $e^-$                 | -1                     | Positron $e^+$  | +1                     | 0.511           | Weak, electromagnetic                         |
| Neutrino $\nu$                 | 0                      | Antineutrino $\bar{\nu}$  | 0                      | 0               | weak  |
| Muon $\mu^-$                   | -1                     | Antimuon $\mu^+$  | +1                     | 106             | Weak, electromagnetic                         |
| Pions<br>$\pi^+, \pi^0, \pi^-$ | +1,0,-1                | $\pi^+$ for a $\pi^-$<br>$\pi^-$ for a $\pi^+$<br>$\pi^0$ for a $\pi^0$ | -1,0,+1                | 140,135,140     | Strong ,electromagnetic<br>( $\pi^+, \pi^-$ ) |

### 1.3.2. Mesons

Mesons are complex and unstable particles because they consist of quarks and anti-quarks. In addition, the median age of the meson is  $2.6 \times 10^{-8}$  s and the mass of the meson is less than the mass of the proton and greater than the mass of the electron. The mesons were discovered by Karl Anderson in 1937. The meson spin is either zero or one true. When the mesons break apart, an electron, positron, neutrino or photon is produced and the charge of the mesons is either positive, negative or neutral. The best example of mesons is the pion, which consists of quarks and anti-quarks .

Table 1.4. *The mesons.*

| Symbol   | Name    | Quark content | Electric charge | Mass GeV/c <sup>2</sup> |
|----------|---------|---------------|-----------------|-------------------------|
| $\pi^+$  | pion    | $u\bar{d}$    | +1              | 0.140                   |
| $K^-$    | kaon    | $s\bar{u}$    | -1              | 0.494                   |
| $\rho^+$ | rho     | $u\bar{d}$    | +1              | 0.770                   |
| $B^0$    | B- zero | $d\bar{b}$    | 0               | 5.279                   |
| $\eta^c$ | eta-c   | $c\bar{c}$    | 0               | 2.980                   |

### 1.4. The Four Forces in Nature

The forces all around the world where we live in today is called the electromagnetic force. This is the force of gravity, in other words, the strong force and known as the weak force.

To begin with, gravity is the weakest force and in that force, while weak and strong force operates in very short distances between primary particles, particles are less than atoms, and the strong force is called the strongest force among the four fundamental forces.

The method of the origin of this force which is by the particles of the carrier of the force, exchanges between the particles and this is called the boson, as the exchange of the boson particles between them lead to the emergence of this energy.

Furthermore, the bosons are divided into four types as follows; the force of gravity carried by Grafton and the electromagnetic force carried by a photon. The weak force is carried by Z.W, while the strong force is matched by gluons.

Since the gravitational effect is weak and can be ignored as the standard model is centred around very small particles, gravity can be neglected, so there is no gravitational force in the standard model.

#### **1.4.1. The electromagnetic force**

The photon is the basic component of electromagnetic and the photon is only a boson in the standard model. It is responsible for carrying the electromagnetic force. The photon is also called the two-wave particle because it combines the properties of both particles and waves. Later it was discovered that the photon is only neutrino and interento and then modified the idea that the photon has no mass, in the early sixties has been proven evidence and experience that neutrons have a very small mass .

#### **1.4.2. The strong force**

It was common that the material was consisted of protons and neutrons only, and scientists were looking at what the force was which carried protons linked inside the nucleus and do not contradict because of the strength of dissonance resulting from the similarity of their charges. On the contrary, in the early 1970s, scientists realized that protons and neutrons were made up of elementary particles called quarks. All of this has led to define what is known as the quantum chromo-dynamic theory.

Throughout this feedback, we come to an understanding that strong nuclear force is the combination of quarks and anti-quarks in the Hadrons that will be mentioned later on this specific paper.

### 1.4.3. The gravity force

Gravity is one of the observed forces that we see every day in our lives because it operates under distances and gravity does not resemble nuclear power, which is a very short range. Moreover, gravity is responsible for our stability on the ground, the stability of buildings and anything we see and experience among us including the earth around the sun and the rotation of the moon around the earth .

In this study, the force of gravity at length will not be covered since the outcomes result in the foundation of the standard model theory, which describes three forces out of four such as electromagnetic, strong and weak. Gravity has not been one of these forces that were mentioned.

### 1.4.4. The weak force

Although the force charged by the boson is more powerful than the gravitational force. It is considered to be weaker than other forces and is effective at very short distances. 1 Beta dissolution is the best example of weak force as shown in the following figure:

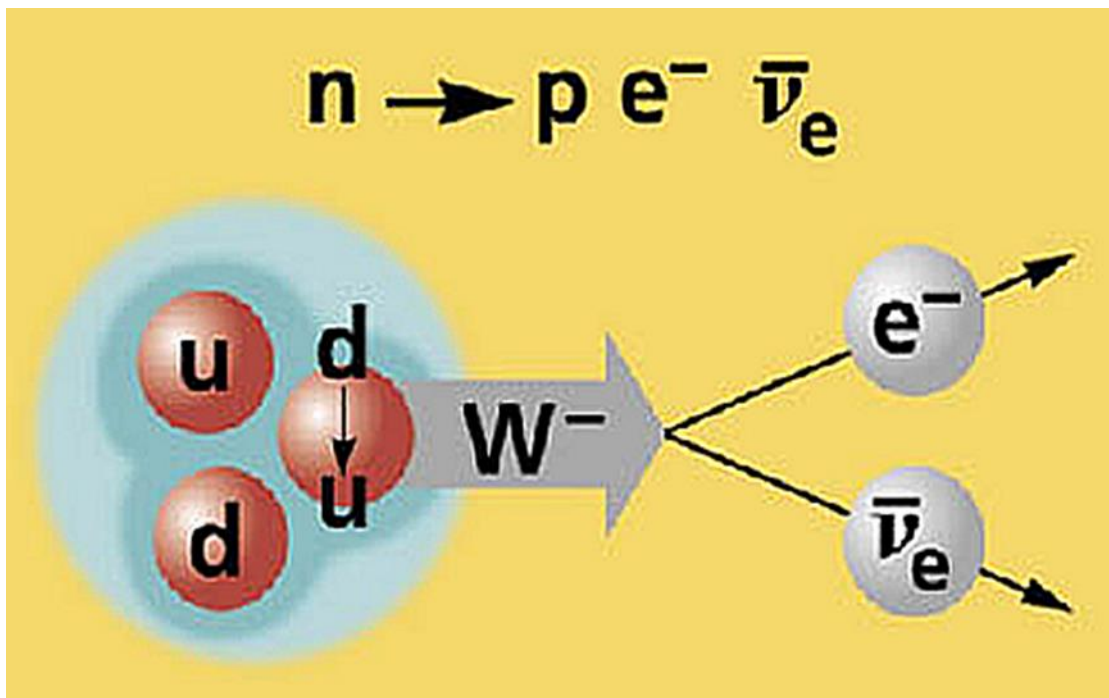


Figure 1.2. Beta dissolution.

## 1.5. Antiparticle

After describing the behaviour of the electron in the electromagnetic field before and after he proposed his theory of relativity, which resulted in two cases can be discussed as the first description of electrons which have been negative while the other was described as the electron positive charge and this idea seemed more of an unusual kind.

However, the 1932 discovery had been like an electron in its properties, but its charge was positive. It was called as Dirac in his theory which was later called antibodies. Particles and Antiparticles could be the atoms and hence the material, this specific material cannot be composed of particles and their antiparticles. If a particle encounters a counterpart of the opposite particle the two will disappear.

The first evidence of the presence of antiparticles was discovered in 1955 by physicists when they used particle accelerators and which also revealed the presence of more than 200 elementary particles.

Table 1.5. *Particle and antiparticle.*

| Particle     | Symbol      | Charge   | Rest mass /MeV  |
|--------------|-------------|----------|-----------------|
| Electron     | $e^-$       | -        | <b>0.510999</b> |
| Positron     | $e^+$       | +        | <b>0.510999</b> |
| Proton       | $p$         | +        | <b>938.257</b>  |
| Antiproton   | $\bar{p}$   | -        | <b>938.257</b>  |
| Neutron      | $n$         | <b>0</b> | <b>939.551</b>  |
| Antineutron  | $\bar{n}$   | <b>0</b> | <b>939.551</b>  |
| Antineutrino | $\bar{\nu}$ | <b>0</b> | <b>0</b>        |
| Neutrino     | $\nu$       | <b>0</b> | <b>0</b>        |



## 1.6. Interactions

Another name given to basic forces is basic interactions that involve both weak and strong interactions which are present in a very small space. These interactions are electromagnetic and are visible which can easily be observed. Physicists have also described the basic interactions as a separate quantum field, which were among the particles given to us by the standard model of particle physics. The gluon particle is well known for the strong interaction, which means that the gluon contributes to the binding of the quarks from where the hadrons are formed. As a result, the radon is connected with each other with the same force as the nucleus of the atom. What makes a weak interaction are the bosons that have been mentioned before. It should also be noted that the photon carries the electromagnetic forces that are stronger than the force of gravity, and this is true only in the short distances while in the vast and massive distances, the force of gravity is dominant.

End of seventies physicists attempted to calculate the magnitude of gravity as the first step in the way of unification of electromagnetic force which were both the unification of electromagnetic interactions and the strong interactions with electroweak theory. It was generally a theoretical proposal combining four interactions with each other as the weak force and the strong force with gravity.

### 1.6.1. Electroweak interactions

The quark can change from one flavor to another through a weak interaction, for instance, in radiation and beta decay, neutrons are divided into electrons and protons, where the down quark is decomposed into an up quark. Thus, the neutrons are converted into protons and the boson is then decomposed into an electron . Strong interaction is the result of the force of attraction and the contrast between the quarks where the gluon carries this force and called the theory that describes this chromo dynamic QCD . The Gluon transfer force between matter particles, which are either mesons, quarks or composite particles of quarks, such as neutrons and protons.

## 1.7. The Standard Model

It should be noted that the standard model theory is incomplete even though it describes several new unexplained phenomena, For instance, scientists have discovered quarks several years ago and yet they cannot accurately identify the upper quark kernels without experimenting because the standard model does not explain the probability of a mass of particles that are uncertain by commercialization .

Therefore, it can be said that the theory of the standard model of particle physics describes all three interactions such as strong, weak and electromagnetic interactions, as this theory passed several stages to develop from 1970 to 2012. After all, this success of the theory of the standard model can be considered the theory of everything. Contains the force of gravity and absolute energy, but it has achieved success theoretically and mathematically .

However, physicists in experimental and theoretical particles have shown great interest in trying to change several strange phenomena, such as the existence of dark matter and in simulation, where they help in new physics and beyond the standard model.

In the last few years, the standard model has been used in several applications along with particle physics such as astrophysics, nuclear physics and cosmology.

**Three Generations of Matter (Fermions)**

|           | I  | II   | III  |                                       |                      |
|-----------|--|--|--|---------------------------------------|----------------------|
| mass→     | 3 MeV  | 1.24 GeV                                     | 172.5 GeV                                    | 0                                     | 125.7 GeV            |
| charge→   | $\frac{2}{3}$                                  | $\frac{2}{3}$                                | $\frac{2}{3}$                                | 0                                     | 0                    |
| spin→     | $\frac{1}{2}$                                  | $\frac{1}{2}$                                | $\frac{1}{2}$                                | 1                                     | 0                    |
| name→     | <b>u</b><br>up                                 | <b>c</b><br>charm                            | <b>t</b><br>top                              | <b><math>\gamma</math></b><br>photon  | <b>H</b><br>Higgs    |
| Quarks    | 6 MeV  | 95 MeV                                       | 4.2 GeV                                      | 0                                     | 0                    |
|           | $-\frac{1}{3}$                                 | $-\frac{1}{3}$                               | $-\frac{1}{3}$                               | 0                                     | 0                    |
|           | $\frac{1}{2}$                                  | $\frac{1}{2}$                                | $\frac{1}{2}$                                | 1                                     | 2                    |
|           | <b>d</b><br>down                               | <b>s</b><br>strange                          | <b>b</b><br>bottom                           | <b>g</b><br>gluon                     | <b>G</b><br>Graviton |
| Leptons   | <2 eV  | <0.19 MeV                                    | <18.2 MeV                                    | 90.2 GeV                              |                      |
|           | 0  | 0  | 0  | 0                                     |                      |
|           | $\frac{1}{2}$                                  | $\frac{1}{2}$                                | $\frac{1}{2}$                                | 1                                     |                      |
|           | <b><math>\nu_e</math></b><br>electron neutrino | <b><math>\nu_\mu</math></b><br>muon neutrino | <b><math>\nu_\tau</math></b><br>tau neutrino | <b><math>Z^0</math></b><br>weak force | Bosons (Forces)      |
| 0.511 MeV | 106 MeV  | 1.78 GeV                                     | 80.4 GeV                                     |                                       |                      |
|           | -1   | -1   | -1   | $\pm 1$                               |                      |
|           | $\frac{1}{2}$                                  | $\frac{1}{2}$                                | $\frac{1}{2}$                                | 1                                     |                      |
|           | <b>e</b><br>electron                           | <b><math>\mu</math></b><br>muon              | <b><math>\tau</math></b><br>tau              | <b><math>W^+</math></b><br>weak force |                      |

Figure 1.3. The standard model of particle physics.

### 1.8. Beyond the Standard Model

Although the standard model and describing the interactions of the material have shown a great success, they form only 4% of the universe and the largest proportion in the unexplained part of the standard model, which is dark energy and dark matter .

## **1.9. The Large Hadron Collider**

To begin with, the Large Hadron Collider (LHC) is a 328-foot underground machine located between the borders of France and Switzerland. It should be known that the Large Hadron Collider is one of the projects undertaken by CERN. Moreover, the Large Hadron Collider is considered one of the largest devices manufactured by man and employs a large number of scientists from different countries of the world. As this Collider propels proton beams close to the speed of light and then collides with these beams. The changes occurring on these beams are recorded by six detectors located on the perimeter of the Large Hadron Collider. In addition, the heart of the Large Hadron Collider the coldest place on earth and the coldest in the world outside the atmosphere. The reason behind the manufacture of such a device that has cost millions of dollars is knowing what is going on around us in every detail, no matter how small.

### **1.9.1. Main detectors in LHC**

The Large Hadron Collider contains several main detectors. These are mentioned below as follow:

#### **1.9.1.1. Atlas Detector**

(A Toroidal LHC Apparatus) the Atlas detector is one of the largest reagents in the LHC but in the world it is well known with a height of 25 meters, a length of 46 meters and a width of 25 meters and a volume of 28750 cubic meters. Inside the detector, there is a device called Inner Tracker, which is responsible for the monitoring and analysis of what happens to protons during the collision and what is produced after the collision. It also has a Calorimeter that can measure particle energy by monitoring particle movement and information by this detector.

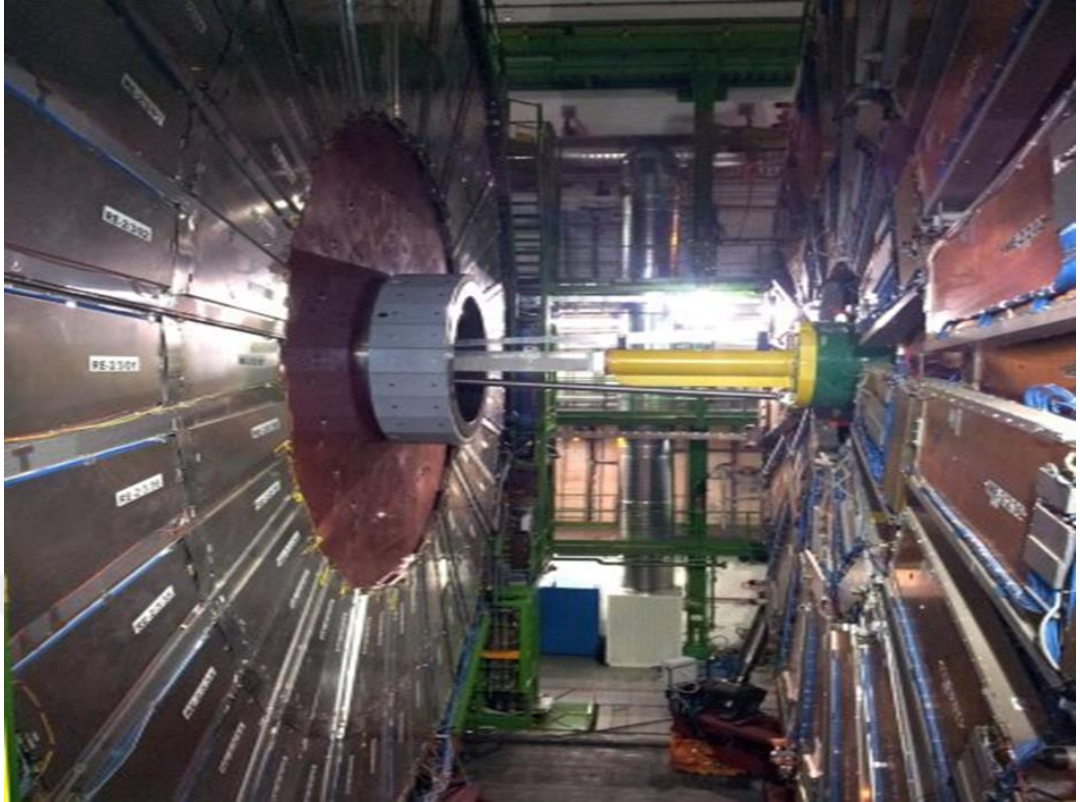


Figure 1.4. A Toroidal LHC Apparatus (Atlas).

#### **1.9.1.2. Detector (CMS)**

CMS is the phrase that is given as short initials for Compact Moun Solenoid. It can be said that this device aims to measure and monitor the initial particles produced after the collision as in the Atlas detector. There is also a very large magnet surrounding the CMS and has a magnetic field greater than the magnetic field of the Earth by 100 thousand times.

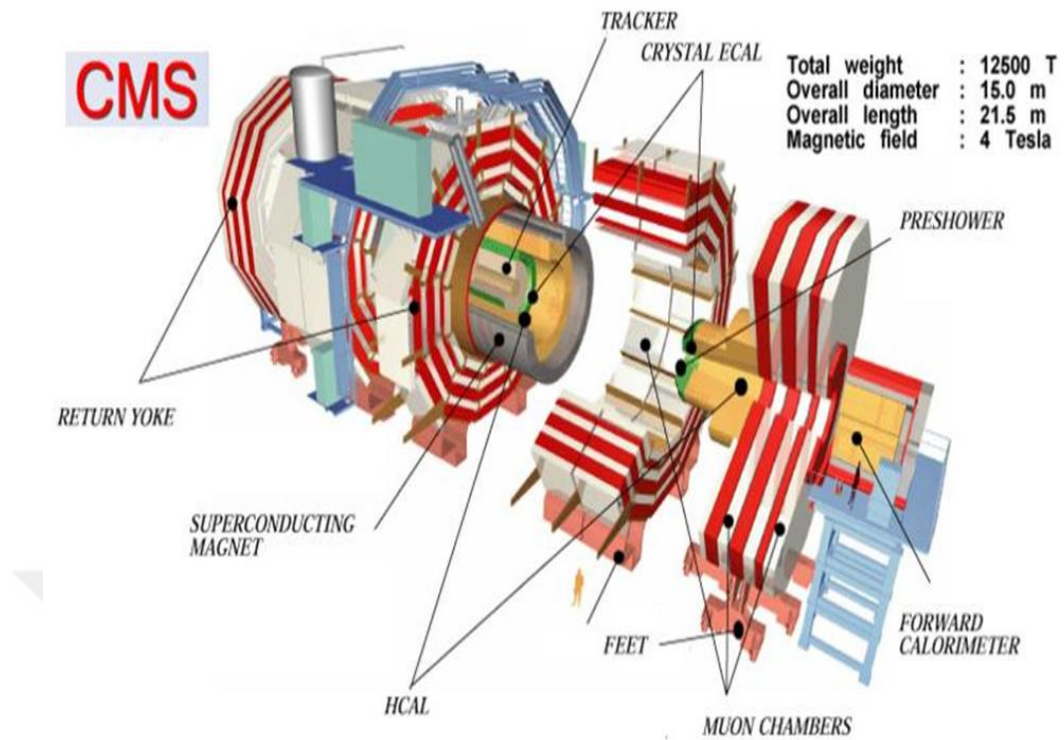


Figure 1.5. Compact Muon Solenoid (CMS).

### 1.9.1.3. Alice Detector (A Large Ion Collider Experiment)

A Large Ion Collider Experiment, It studies the collisions between heavy ions. The Alice detector contains the time projection chamber TPC.

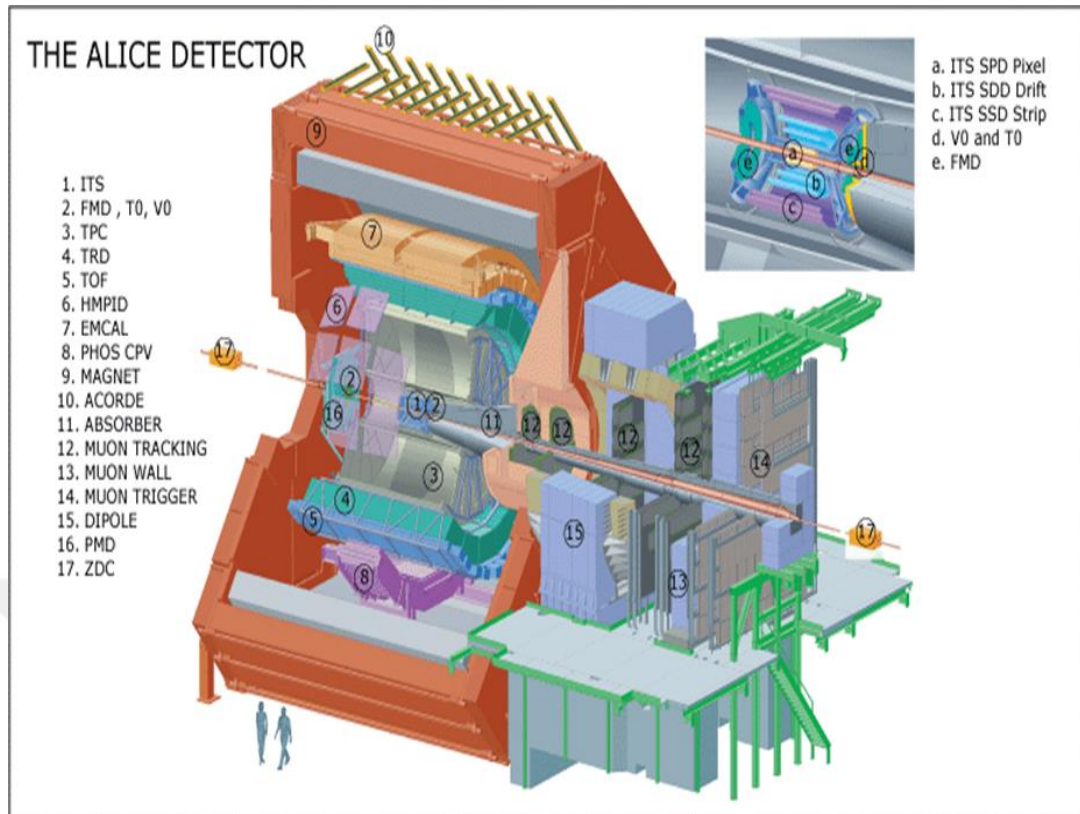


Figure 1.6. A Large Ion Collider Experiment (Alice).

#### 1.9.1.4. Beauty Detector: Large Hadron Collider

This detector is designed to know the difference between the material we know and the dark matter, by searching for the quarks of beauty.

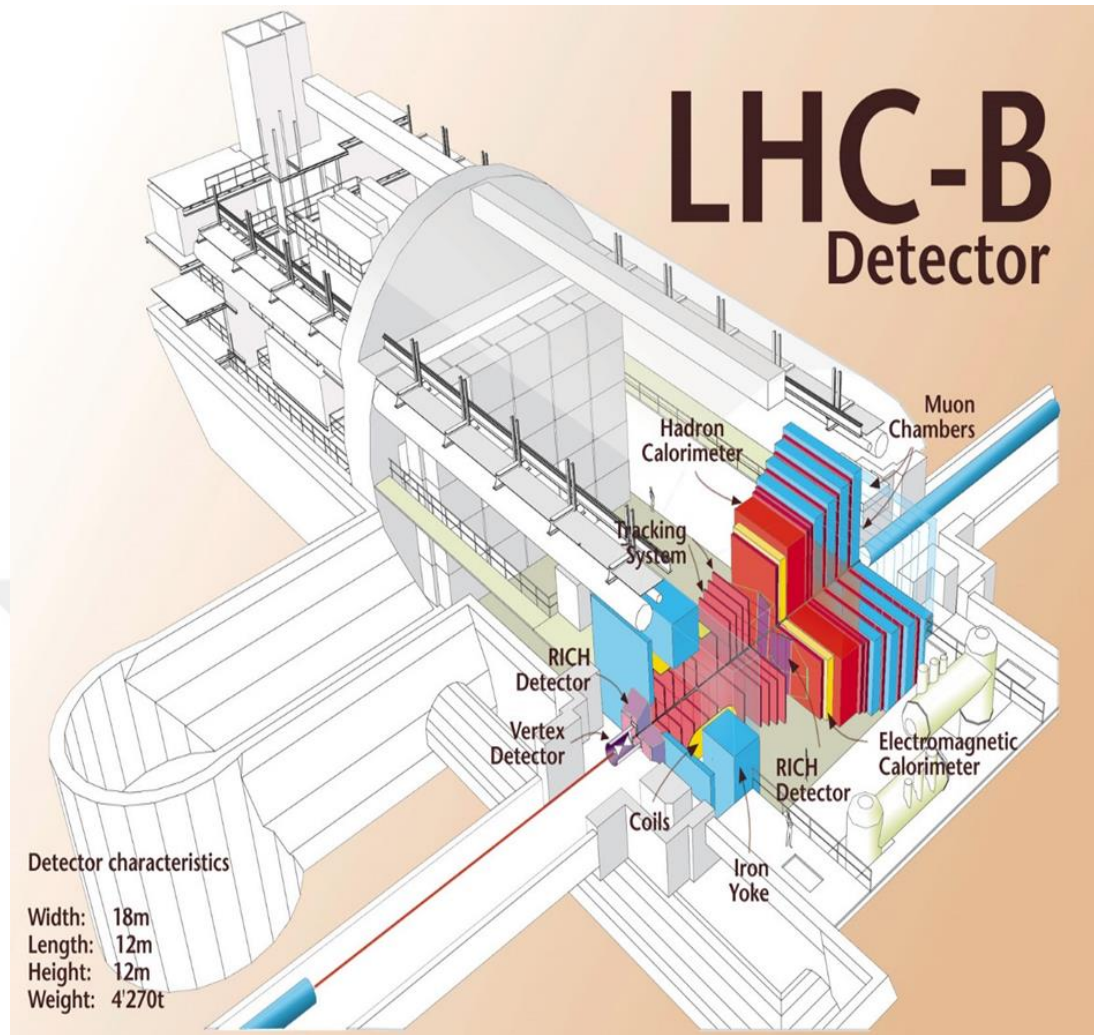


Figure 1.7 Large Hadron Collider Beauty (LHC-B).

There are also two small detectors within the Large Hadron Collider (LHC) which are abbreviations for the Great Hadron Collider and the other named as Totem which is the total measure of a flexible and zoological (cross-section). It is also aimed to highlight that there are also thousands of scientists working on each of these detectors.

## 1.9.2. How the Large Hadron Collider Works:

### 1.9.2.1. Acceleration

At first, protons must be present separately to be accelerated by the device. Protons can be obtained separately by separating the electrons from the hydrogen atoms.



The protons then enter the accelerator called the PS Baster, where the protons are accelerated within it to reach the appropriate speed and energy and then driven by the accelerator PS activator to the accelerator SPS is the accelerator of the super-protons, and then split all the packages so that each proton on its own, At this moment the speed of each Proton is approximately the same speed of light and then the accelerator SPS push these beams to the large Hadron Collider and this is through two tubes, One moving clockwise and the other counterclockwise and at that moment the speed of each proton the same speed of light is almost Each proton is flipped in the tube surrounding the large Hadron Collider 11245 A roll in the second.

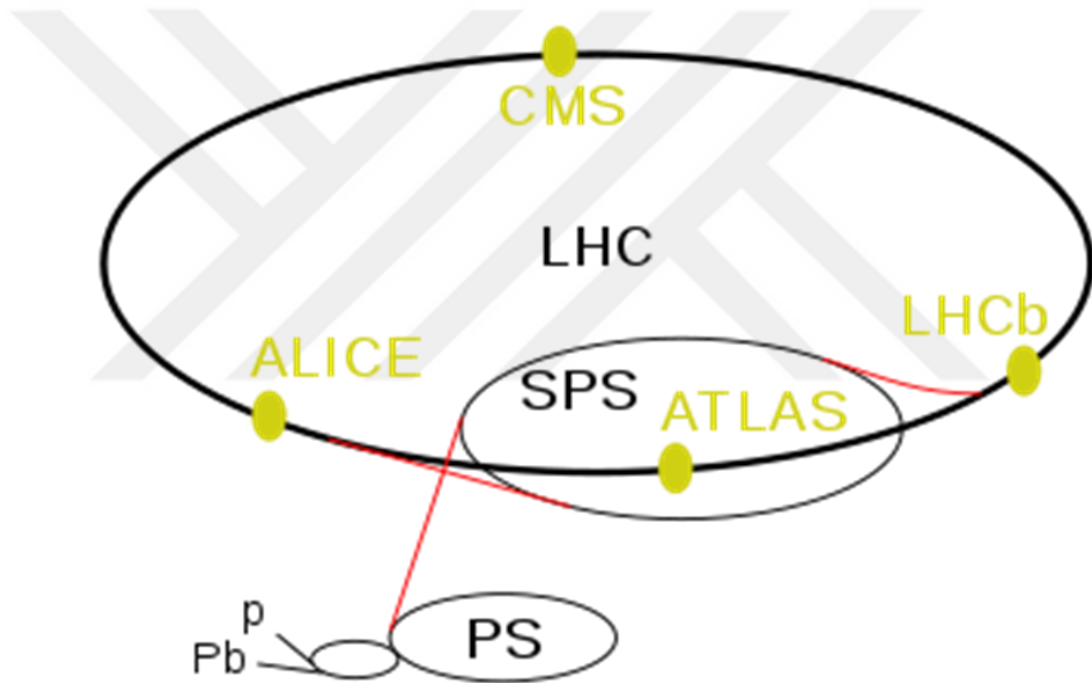


Figure 1.8. The accelerators in The Large Hadron Collider (LHC).

### 1.9.2.2. Collision

First of all, after the passage of protons within the two tubes come from the accelerator they go out as follows and since the movement of each other inverse pack, each contain a large number of protons move at the speed of light. It occurs about 600 million collisions per second where every proton coming from a tube Collides with the proton coming from the opposite tube and then divided into smaller particles, quarks, and a force known as muon begins. As we have said before, the quarks are not stable and therefore they have even faded and decompose into new particles. Here it is aimed to point out that the work of Large Hadron Collider cannot force all righteousness and therefore there are a number of protons continue to move without resistance or collision with any proton in the opposite direction and at the end of the path there is a part of the device that is made of graphite where it absorbs the remaining package of protons and then are added to this part of the device to protect Large Hadron Collider. If there is an error in the package path or the collision has lost control of the package.

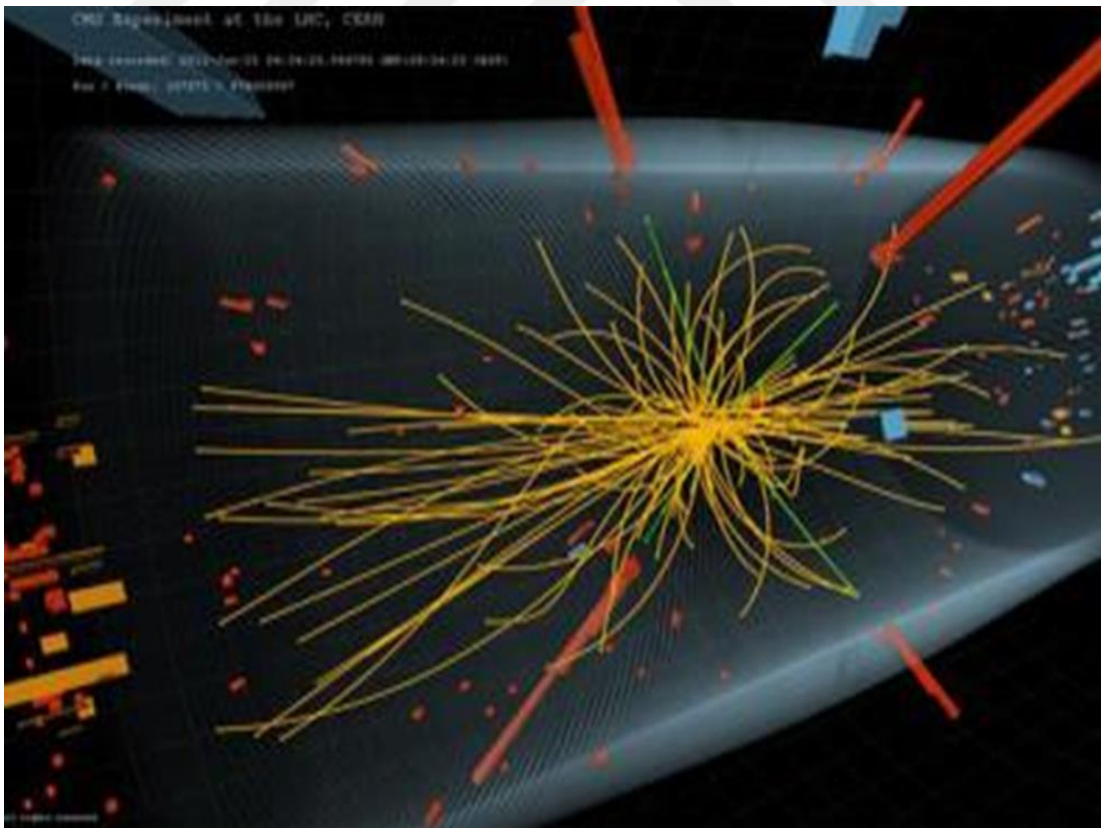


Figure 1.9. The form of collisions within the Large Hadron Collider.

### 1.9.2.3. Data and results of the Large Hadron Collider

After collecting the data from the reagents in the Large Hadron Collider, it is estimated to be at about 15 million gigabytes and then these data are divided and later each part is sent to a computer. After the computers process this data, they are all sent to a central computer which is called Grid Computing where scientists analyze this information and the results to be used in the understanding of the universe and maidur around us has been revealed such information on the standard model of physical particles and Higgs boson also discovered that the neutrons do not have a mass. It is a point to highlight that scientists also try to answer several questions that the standard model could not answer such as dark matter and other questions that puzzled humans.



Figure 1.10. Computers in the Large Hadron Collider.



Figure 1.11. Computing Center - CERN.

## 2. CALCULATIONS

### 2.1. Introduction

The standard model gives us a brief idea of all the information we need to know about strong interactions and weak interactions in addition to electromagnetic interactions, but this theory has not been effective in answering many of the questions. But by discovering a number of new fermions we can reduce the number of questions Unknown by the standard model We could produce new heavy quarks in pairs at the Hadron collider large at the center of mass energy 13 TeV. However, due to the foreseeable smallness of the mixing between the new heavy quarks and known quarks, the decay modes can be perfectly different from the one relevant to charged weak interactions. A new symmetry beyond the SM is expected to explain the smallness of these mixings. Anomalous interactions of the top quark are more valid for the new heavy quarks  $t'$  and  $b'$  due to their expected larger masses than the top quark.

The fourth family quarks were also studied through anomalous interactions at LHC. For example, ATLAS experiment and CMS experiment have been experimenting with the fourth generation of quarks, The ATLAS experience has contributed to the possibility of producing a pair of new quarks and vector-like quarks, so it put limits as 760 GeV for the current neutral channel and 900 GeV for the current channel Charged at  $\sqrt{s} = 7$  TeV.

In this thesis, we introduce the analysis of anomalous productions and decay of new heavy quarks  $t'$  at LHC. We have carried out the fast simulation for the background and signal. Any noting of the invariant mass peak in the range of 300 – 1000 GeV and excess in the events with the final states originating from  $t' V$  can be interpreted as the signal for the new heavy quark  $t'$  by means of the interactions of anomalous.

## 2.2. The Anomalous Interactions Through The Heavy Quarks

A general theory that encompassing the standard model (SM) as its low energy limit can be written as an expansion series in power of  $\Lambda^{-1}$  with operators comply the wanted symmetries.

For research the influential Lagrangian for the anomalous interactions between the new heavy quarks ( $Q = t$ ), normal quarks and the gauge bosons ( $V = \gamma, Z, g$ ) can be formulated as,

$$L = \sum_{q_i=u,c,t} \frac{k_\gamma^{qi}}{\Lambda} Q_{qi} g_e t^{-1} \sigma_{\mu\nu} q_i F^{\mu\nu} + \sum_{q_i=u,c,t} \frac{k_z^{qi}}{2\Lambda} g_z t^{-1} \sigma_{\mu\nu} q_i Z^{\mu\nu} + \sum_{q_i=u,c,t} \frac{k_g^{qi}}{2\Lambda} g_s t^{-1} \sigma_{\mu\nu} \lambda_a q_i G^{\mu\nu} G_a^{\mu\nu} \quad (2.1)$$

Where,  $\sigma_{\mu\nu} = i(\gamma_\mu \gamma_\nu - \gamma_\nu \gamma_\mu)/2$ ;  $\lambda_a$  are the Gell-Mann matrices,  $G^{\mu\nu}$ ,  $F^{\mu\nu}$  and  $Z^{\mu\nu}$  are the field strength tensors of the gauge bosons,  $Q_q$  is the electric charge of the quark ( $q$ );  $g_z$ ,  $g_e$  and  $g_s$  are neutral weak, electromagnetic and the strong conjugation constants, respectively. Where,  $g_e = \cos \theta_w \sin \theta_w$ . Where,  $\theta_w$  is the weak mixing angle, this means that the electromagnetic conjugation constant, depending on neutral weak conjugation constant. There is also  $k_z$  is the anomalous conjugation with boson;  $k_\gamma$  is the anomalous conjugation with photon and  $k_g$  for gluon. At last  $\Lambda$  is the cutoff scale for the new interactions.

### 2.3. Decay Widths And Branchings

With regard to the decay channels  $Q \rightarrow V q$  where, ( $V = g, \gamma, Z$ ), we calculate the anomalous decay widths using the influential Lagrangian as described below:

$$\Gamma(Q' \rightarrow gq) = \frac{2}{3} \left( \frac{k_g^q}{\Lambda} \right)^2 \alpha_s m_{Q'}^3 \lambda_0 \quad (2.2)$$

$$\Gamma(Q' \rightarrow \gamma q) = \frac{2}{3} \left( \frac{k_g^q}{\Lambda} \right)^2 \alpha_s m_{Q'}^3 \lambda_0 \quad (2.3)$$

$$\Gamma(Q' \rightarrow Zq) = \frac{1}{16} \left( \frac{k_Z^q}{\Lambda} \right)^2 \frac{\alpha_e m_{Q'}^3}{\sin^2 \theta_w \cos^2 \theta_w} \lambda_Z \sqrt{\lambda_r} \quad (2.4)$$

$$\lambda_0 = 1 - \frac{3m_q^2}{m_{Q'}^2} + \frac{3m_q^4}{m_{Q'}^4} - \frac{m_q^6}{m_{Q'}^6} \quad (2.5)$$

With

$$\lambda_r = 1 + \frac{m_w^4}{m_{Q'}^4} + \frac{m_q^4}{m_{Q'}^4} - \frac{2m_w^2}{m_{Q'}^2} - \frac{2m_q^2}{m_{Q'}^2} - \frac{2m_w^2 m_q^2}{m_{Q'}^4} \quad (2.6)$$

$$\lambda_Z = 2 - \frac{m_Z^2}{m_{Q'}^2} - \frac{4m_q^2}{m_{Q'}^2} + \frac{2m_q^4}{m_{Q'}^4} - \frac{6m_q m_Z^2}{m_{Q'}^3} - \frac{m_Z^2 m_t^2}{m_{Q'}^4} - \frac{m_Z^4}{m_{Q'}^4} \quad (2.7)$$

The anomalous decay widths in diverse channels are varied to  $\Lambda^{-2}$ , and they are presumed for  $k/\Lambda > 0.1$  TeV over the charged present channels. In this status, it is clear that if we use the anomalous conjugation then the branching rates will be almost independent of  $k/\Lambda$ . We have utilized three parameterizations groups, which we called PI, PII and PIII. We postulate the fixed value  $k/\Lambda=0.01$  TeV for PI,  $k/\Lambda = 0.1$  TeV for PII and  $k/\Lambda = 0.5$  TeV for PIII.

The following three tables show the decay width and branching rates of the new heavy quark  $t'$  through anomalous interactions for PI, PII and PIII, respectively.

Table 2.1. *Branching rates (%) and decay widths of the heavy  $t$  quark for PI.*

| Mass (GeV) | $\gamma_{c(u)} \%$ | $\gamma_{t\%}$ | $z_{c(u)} \%$ | $z_t \%$ | $g_{c(u)} \%$ | $g_{t\%}$ | W <sub>bp</sub> % | W <sub>d</sub> % | W <sub>b</sub> % | W <sub>s</sub> % | $\Gamma$ (GeV) |
|------------|--------------------|----------------|---------------|----------|---------------|-----------|-------------------|------------------|------------------|------------------|----------------|
| 300        | 0.00087            | 0.00025        | 0.0024        | 0.00026  | 0.039         | 0.011     | 0                 | 0.032            | 79               | 21               | 0,54           |
| 400        | 0.00086            | 0.00046        | 0.0024        | 0.0011   | 0.039         | 0.021     | 0                 | 0.032            | 79               | 21               | 1.29           |
| 500        | 0.00086            | 0.00058        | 0.0026        | 0.0016   | 0.039         | 0.026     | 0                 | 0.031            | 79               | 21               | 2.54           |
| 600        | 0.00086            | 0.00066        | 0.0026        | 0.0019   | 0.038         | 0.031     | 0                 | 0.031            | 79               | 21               | 4.39           |
| 700        | 0.00085            | 0.00071        | 0.0026        | 0.0021   | 0.038         | 0.032     | 0                 | 0.031            | 79               | 21               | 6.97           |
| 800        | 0.00085            | 0.00074        | 0.0027        | 0.0023   | 0.038         | 0.033     | 0                 | 0.031            | 79               | 21               | 10.41          |
| 900        | 0.00085            | 0.00076        | 0.0027        | 0.0024   | 0.038         | 0.034     | 0                 | 0.031            | 79               | 21               | 14.82          |
| 1000       | 0.00085            | 0.00078        | 0.0027        | 0.0024   | 0.038         | 0.035     | 0                 | 0.031            | 79               | 21               | 20.33          |



According to the results in Table 2.1, the decay width and branching rates of the new heavy quark  $t'$  by taking the anomalous coupling  $k/\Lambda = 0.01$  TeV We calculate the  $\Gamma$  (  $\Gamma = 0.54, 4.39$  and  $20.33$  GeV ) for  $m_{t'} = 300$  GeV,  $600$  GeV and  $1000$  GeV respectively. It is also the lowest value of the branching with  $t' \rightarrow q\gamma$  While the largest value of the branching with  $t' \rightarrow W$ . The table also shows that the values of the decay display are increasing as the mass increases.

As we can observe in table (2.2), the decay width and branching rates of the new heavy quark  $t'$  by taking the anomalous coupling  $k/\Lambda = 0.1$  TeV We calculate the  $t'$  decay width, (  $\Gamma = 0.59, 4.9$  and  $23$  GeV ) for  $m_{t'} = 300$  GeV,  $600$  GeV and  $1000$  GeV , respectively. The table also shows that the values of the decay widths are increasing as the mass increases.

Table 2.2. Branching rates (%) and decay widths of the heavy  $t$  quark for  $PII$ .

| Mass (GeV) | $\gamma_{c(u)} \%$ | $\gamma_t \%$ | $z_{c(u)} \%$ | $z_t \%$ | $g_{c(u)} \%$ | $g_t \%$ | Wbp% | Wd%   | Wb | Ws% | $\Gamma(\text{GeV})$ |
|------------|--------------------|---------------|---------------|----------|---------------|----------|------|-------|----|-----|----------------------|
| 300        | 0.079              | 0.023         | 0.22          | 0.024    | 3.6           | 1        | 0    | 0.029 | 72 | 19  | 0.59                 |
| 400        | 0.078              | 0.041         | 0.23          | 0.1      | 3.5           | 1.9      | 0    | 0.029 | 71 | 19  | 1.4                  |
| 500        | 0.077              | 0.052         | 0.23          | 0.15     | 3.5           | 2.3      | 0    | 0.028 | 71 | 19  | 2.8                  |
| 600        | 0.077              | 0.059         | 0.23          | 0.17     | 3.5           | 2.6      | 0    | 0.028 | 71 | 19  | 4.9                  |
| 700        | 0.077              | 0.063         | 0.24          | 0.19     | 3.4           | 2.8      | 0    | 0.028 | 70 | 19  | 7.8                  |
| 800        | 0.076              | 0.066         | 0.24          | 0.2      | 3.4           | 3        | 0    | 0.028 | 70 | 19  | 12                   |
| 900        | 0.076              | 0.068         | 0.24          | 0.21     | 3.4           | 3.1      | 0    | 0.028 | 70 | 19  | 17                   |
| 1000       | 0.076              | 0.07          | 0.24          | 0.22     | 3.4           | 3.1      | 0    | 0.028 | 70 | 19  | 23                   |

Table 2.3. Branching rates (%) and decay widths of the heavy  $t$  quark for PIII.

| Mass (GeV) | $\gamma_c(u)$ % | $\gamma_t$ % | $z_c(u)$ % | $z_t$ % | $g_c(u)$ % | $g_t$ % | Wbp% | Wd%    | Wb | Ws% | $\Gamma$ (GeV) |
|------------|-----------------|--------------|------------|---------|------------|---------|------|--------|----|-----|----------------|
| 300        | 0.64            | 0.19         | 1.7        | 0.19    | 29         | 8.3     | 0    | 0.0092 | 23 | 6.2 | 1.8            |
| 400        | 0.59            | 0.31         | 1.7        | 0.76    | 26         | 14      | 0    | 0.0086 | 22 | 5.8 | 4.7            |
| 500        | 0.56            | 0.38         | 1.7        | 1.1     | 25         | 17      | 0    | 0.0083 | 21 | 5.6 | 9.6            |
| 600        | 0.55            | 0.42         | 1.7        | 1.2     | 25         | 19      | 0    | 0.0081 | 20 | 5.4 | 17             |
| 700        | 0.54            | 0.45         | 1.7        | 1.3     | 24         | 20      | 0    | 0.008  | 20 | 5.3 | 28             |
| 800        | 0.53            | 0.46         | 1.7        | 1.4     | 24         | 21      | 0    | 0.0079 | 20 | 5.3 | 42             |
| 900        | 0.53            | 0.47         | 1.7        | 1.5     | 24         | 21      | 0    | 0.0078 | 20 | 5.2 | 60             |
| 1000       | 0.53            | 0.48         | 1.7        | 1.5     | 24         | 22      | 0    | 0.0078 | 19 | 5.2 | 82             |

According to values are obtained in Table (2.3), we can observe that, the decay width and branching rates of the new heavy quark  $t'$  by taking the anomalous coupling  $\kappa/\Lambda = 0.5$  TeV olarak alındığında; , We calculate the  $t'$  decay width, ( $\Gamma = 1.8, 17$  and  $82$  GeV ) for  $m_{t'} = 300$  GeV,  $600$  GeV and  $1000$  GeV, respectively. The table also shows that the values of the decay display are increasing as the mass increases.

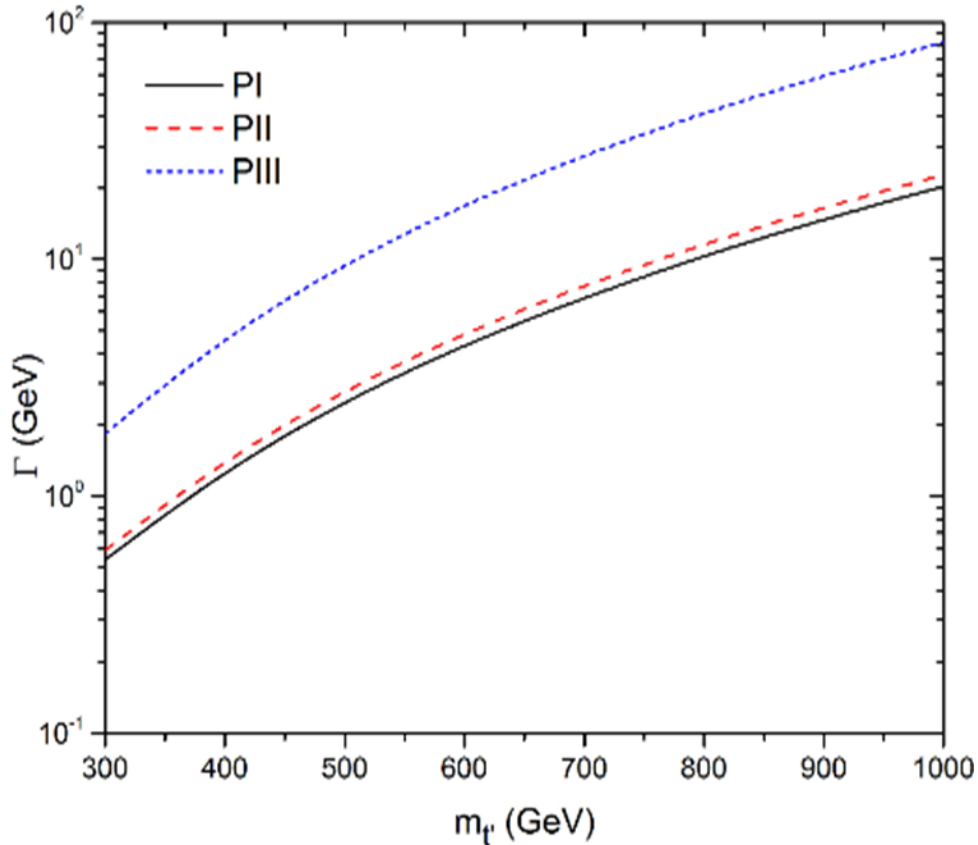


Figure 2.1 Total decay width of  $t'$  depending on its mas

Considering the Figure (2.1), we conclude that the relationship between the decay width and the mass for  $pp \rightarrow Vq$  where ( $V = \gamma, G, Z$ ) and  $q = (c, u)$  as it shows that the decay width is increasing as the mass increases for PI, PII and PIII.

#### 2.4. The cross sections and analysis of the process $pp \rightarrow W^+ bV^+ X$ for $t'$ signal

The cross sections means a measurement that reveals the likelihood that a particular result will be produce. Therefore, we simulated the method of production and new heavy quarks at LHC and using efficient anomalous interaction summits and executed

into the com HEP bundle. Total cross sections for  $t'$  signal ( $\sigma_{\text{Tot}}$ ) are given in table (2.4), with the center of mass energy  $\sqrt{S} = 14$  TeV. For instance, taking the mass of new heavy quark as 500 GeV the cross section of  $t'$  production is calculated as 25.7 pb at the center of mass energy  $\sqrt{S}=14$  TeV for parametrization PIII. It is showing in the table (2.4), the cross sections for  $t'$  signal increase as the mass of the new heavy quark increase.

Table 2.4. Total cross sections for  $t'$  signal at the center of mass energy  $\sqrt{S}=14$  TeV

| $m_{t'}(\text{GeV})$ | $\sigma_{\text{Tot}}(\text{pb})$ |       |      |
|----------------------|----------------------------------|-------|------|
|                      | PI                               | PII   | PIII |
| 300                  | $3.12 \times 10^{-01}$           | 6.34  | 52.2 |
| 400                  | $2.67 \times 10^{-01}$           | 4.65  | 35.4 |
| 500                  | $2.24 \times 10^{-01}$           | 3.41  | 25.7 |
| 600                  | $1.89 \times 10^{-01}$           | 2.56  | 19.9 |
| 700                  | $1.60 \times 10^{-01}$           | 1.94  | 15.7 |
| 800                  | $1.37 \times 10^{-01}$           | 1.45  | 12.7 |
| 900                  | $1.17 \times 10^{-01}$           | 1.14  | 11   |
| 1000                 | $1.00 \times 10^{-01}$           | 0.934 | 9.80 |

Total cross sections for the backgrounds ( $\sigma_{\text{Tot}}$ ) are given in table ( 2.5 ), with the center of mass energy  $\sqrt{S} = 14$  TeV. For instance, taking the mass of new heavy quark as 500 GeV the cross section of  $t'$  production is calculated as  $7.61 \times 10^{-04}$  pb at the center of mass energy  $\sqrt{S}=14$  TeV for parametrization PIII. It is showing in the table ( 2.5 ), the cross sections for the backgrounds increase as the mass of the new heavy quark increase.

Table 2.5. Total cross sections for the backgrounds at the center of mass energy of  $\sqrt{S}=14$  TeV.

| $m_{t'}$ (GeV) | $\sigma_{\text{Tot}}(\text{pb})$ |                        |                        |
|----------------|----------------------------------|------------------------|------------------------|
|                | PI                               | PII                    | PIII                   |
| 300            | $2.80 \times 10^{-04}$           | $2.86 \times 10^{-04}$ | $8.79 \times 10^{-04}$ |
| 400            | $2.38 \times 10^{-04}$           | $2.57 \times 10^{-04}$ | $8.50 \times 10^{-04}$ |
| 500            | $2.00 \times 10^{-04}$           | $2.23 \times 10^{-04}$ | $7.61 \times 10^{-04}$ |
| 600            | $1.63 \times 10^{-04}$           | $1.80 \times 10^{-04}$ | $6.33 \times 10^{-04}$ |
| 700            | $1.32 \times 10^{-04}$           | $1.47 \times 10^{-04}$ | $5.33 \times 10^{-04}$ |
| 800            | $1.07 \times 10^{-04}$           | $1.25 \times 10^{-04}$ | $4.31 \times 10^{-04}$ |
| 900            | $8.75 \times 10^{-05}$           | $1.01 \times 10^{-04}$ | $3.61 \times 10^{-04}$ |
| 1000           | $7.13 \times 10^{-05}$           | $8.16 \times 10^{-05}$ | $2.98 \times 10^{-04}$ |

The signal process  $pp \rightarrow W+ bV+ X$  ( $V = g, Z, \gamma$ ) encompasses the  $t$  interactions in both the s-channel and t-channel. The t-channel gives the non-resonant contribution, while the s-channel contribution to the signal process value in the  $WbV$  invariant mass.

We have acquired the cross sections by using the pseudorapidity cuts  $|\eta_{j,\gamma}| < -2.5$  and transverse momentum cuts  $P_T = 50$  GeV for jets and photon. The signal cross sections depending on the  $t'$  masses for each channel in  $pp \rightarrow \gamma b$  process with pseudorapidity cuts  $|\eta_{j,\gamma}| < -2.5$  and transverse momentum cuts  $P_T = 50$  GeV for PI, PII and PIII is given in table (2.6), table (2.7) and table (2.8), respectively at the center of mass energy  $\sqrt{S}=14$  TeV.

Table 2.6. The cross sections (in pb) for  $t'$  signal at the process  $pp \rightarrow \gamma b$  with  $|\eta_{j,\gamma}| < -2.5$  and  $P_T = 50$  GeV at the center of mass energy  $\sqrt{S} = 14$  TeV for parametrization PI.

| $m_{t'}$ (GeV) | $ug \rightarrow \gamma b$ | $cg \rightarrow \gamma b$ | $gu \rightarrow \gamma b$ | $gu \rightarrow \gamma b$ | $\sigma_{\text{Tot}}(\text{pb})$ |
|----------------|---------------------------|---------------------------|---------------------------|---------------------------|----------------------------------|
| 300            | $3.80 \times 10^{-04}$    | $3.46 \times 10^{-05}$    | $3.80 \times 10^{-04}$    | $3.45 \times 10^{-05}$    | $8.30 \times 10^{-04}$           |
| 400            | $3.13 \times 10^{-04}$    | $2.46 \times 10^{-05}$    | $3.12 \times 10^{-04}$    | $2.46 \times 10^{-05}$    | $6.74 \times 10^{-04}$           |
| 500            | $2.61 \times 10^{-04}$    | $1.80 \times 10^{-05}$    | $2.62 \times 10^{-04}$    | $1.81 \times 10^{-05}$    | $5.59 \times 10^{-04}$           |
| 600            | $2.25 \times 10^{-04}$    | $1.36 \times 10^{-05}$    | $2.25 \times 10^{-04}$    | $1.36 \times 10^{-05}$    | $4.78 \times 10^{-04}$           |
| 700            | $1.97 \times 10^{-04}$    | $1.05 \times 10^{-05}$    | $1.97 \times 10^{-04}$    | $1.05 \times 10^{-05}$    | $4.14 \times 10^{-04}$           |
| 800            | $1.74 \times 10^{-04}$    | $8.24 \times 10^{-06}$    | $1.74 \times 10^{-04}$    | $8.25 \times 10^{-06}$    | $3.64 \times 10^{-04}$           |
| 900            | $1.56 \times 10^{-04}$    | $6.61 \times 10^{-06}$    | $1.55 \times 10^{-04}$    | $6.97 \times 10^{-06}$    | $3.25 \times 10^{-04}$           |
| 1000           | $1.38 \times 10^{-04}$    | $5.42 \times 10^{-06}$    | $1.36 \times 10^{-04}$    | $5.24 \times 10^{-06}$    | $2.85 \times 10^{-04}$           |

Table 2.7. The cross sections for  $t'$  signal at the process  $pp \rightarrow \gamma b$  with  $P_T = 50$  GeV and cuts  $|\eta_{j,\gamma}| < -2.5$  at the center of mass energy  $\sqrt{S} = 14$  TeV for parametrization PII.

| $m_{t'}$ (GeV) | $ug \rightarrow \gamma b$ | $cg \rightarrow \gamma b$ | $gu \rightarrow \gamma b$ | $gu \rightarrow \gamma b$ | $\sigma_{\text{Tot}}(\text{pb})$ |
|----------------|---------------------------|---------------------------|---------------------------|---------------------------|----------------------------------|
| 300            | $6.49 \times 10^{-03}$    | $3.08 \times 10^{-03}$    | $6.53 \times 10^{-03}$    | $3.10 \times 10^{-03}$    | $1.92 \times 10^{-02}$           |
| 400            | $4.90 \times 10^{-03}$    | $2.19 \times 10^{-03}$    | $4.85 \times 10^{-07}$    | $2.31 \times 10^{-03}$    | $9.40 \times 10^{-03}$           |
| 500            | $3.69 \times 10^{-03}$    | $1.60 \times 10^{-03}$    | $3.60 \times 10^{-03}$    | $1.62 \times 10^{-03}$    | $1.05 \times 10^{-02}$           |
| 600            | $2.79 \times 10^{-03}$    | $1.18 \times 10^{-03}$    | $2.78 \times 10^{-03}$    | $1.21 \times 10^{-03}$    | $7.96 \times 10^{-03}$           |
| 700            | $2.16 \times 10^{-03}$    | $8.97 \times 10^{-03}$    | $2.17 \times 10^{-03}$    | $9.18 \times 10^{-04}$    | $6.15 \times 10^{-03}$           |
| 800            | $1.66 \times 10^{-03}$    | $7.02 \times 10^{-04}$    | $1.71 \times 10^{-03}$    | $7.20 \times 10^{-04}$    | $4.79 \times 10^{-03}$           |
| 900            | $1.41 \times 10^{-03}$    | $5.57 \times 10^{-04}$    | $1.43 \times 10^{-03}$    | $5.58 \times 10^{-04}$    | $3.96 \times 10^{-03}$           |
| 1000           | $1.42 \times 10^{-03}$    | $4.96 \times 10^{-04}$    | $1.27 \times 10^{-03}$    | $4.70 \times 10^{-04}$    | $3.66 \times 10^{-03}$           |

Table 2.8. *The cross sections for  $t'$  signal at the process  $pp \rightarrow \gamma b$  with  $P_T = 50$  GeV and cuts  $|\eta_{j,\gamma}| < -2.5$  at the center of mass energy 14 TeV for parametrization PIII.*

| $m_{t'}$ (GeV) | $ug \rightarrow \gamma b$ | $cg \rightarrow \gamma b$ | $gu \rightarrow \gamma b$ | $gu \rightarrow \gamma b$ | $\sigma_{\text{Tot}}(\text{pb})$ |
|----------------|---------------------------|---------------------------|---------------------------|---------------------------|----------------------------------|
| 300            | $5.33 \times 10^{-02}$    | $2.58 \times 10^{-02}$    | $5.36 \times 10^{-02}$    | $2.60 \times 10^{-02}$    | 0.159                            |
| 400            | $3.55 \times 10^{-02}$    | $1.67 \times 10^{-02}$    | $3.68 \times 10^{-02}$    | $1.70 \times 10^{-02}$    | 0.106                            |
| 500            | $2.68 \times 10^{-02}$    | $1.24 \times 10^{-02}$    | $2.98 \times 10^{-02}$    | $1.23 \times 10^{-02}$    | $8.13 \times 10^{-02}$           |
| 600            | $2.30 \times 10^{-02}$    | $1.03 \times 10^{-02}$    | $2.45 \times 10^{-02}$    | $9.77 \times 10^{-03}$    | $6.76 \times 10^{-02}$           |
| 700            | $2.21 \times 10^{-02}$    | $8.59 \times 10^{-03}$    | $1.88 \times 10^{-02}$    | $8.14 \times 10^{-03}$    | $5.76 \times 10^{-02}$           |
| 800            | $2.11 \times 10^{-02}$    | $7.80 \times 10^{-03}$    | $2.05 \times 10^{-02}$    | $7.83 \times 10^{-03}$    | $5.72 \times 10^{-02}$           |
| 900            | $2.16 \times 10^{-02}$    | $8.38 \times 10^{-03}$    | $2.20 \times 10^{-02}$    | $8.30 \times 10^{-03}$    | $6.03 \times 10^{-02}$           |
| 1000           | 0.0240                    | $9.21 \times 10^{-03}$    | 0.0231                    | $9.01 \times 10^{-03}$    | 0.0653                           |

The signal cross sections depending on the  $t'$  masses for each channel in  $pp \rightarrow \gamma b$  process with cuts  $|\eta_{j,\gamma}| < -2.5$  and transverse momentum cuts  $P_T = 50$  GeV for PI, PII and PIII is given in table (2.9), table (2.10) and table (2.11), respectively at the center of mass energy  $\sqrt{s} = 14$  TeV.



Table 2.9. The cross sections for  $t'$  signal at the process  $pp \rightarrow gb$  with  $P_T = 50$  GeV and cuts  $|\eta_{j,\gamma}| < -2.5$  at the center of mass energy 14 TeV for parametrization PI

| $m_{t'}$ (GeV) | $ug \rightarrow gb$    | $cg \rightarrow gb$    | $gu \rightarrow g b$   | $gu \rightarrow g b$   | $\sigma_{Tot}(\text{pb})$ |
|----------------|------------------------|------------------------|------------------------|------------------------|---------------------------|
| 300            | 0.142                  | $1.10 \times 10^{-02}$ | $1.42 \times 10^{-01}$ | $1.09 \times 10^{-02}$ | 0.306                     |
| 400            | 0.123                  | $7.75 \times 10^{-03}$ | $1.23 \times 10^{-01}$ | $7.78 \times 10^{-03}$ | 0.261                     |
| 500            | 0.104                  | $5.56 \times 10^{-03}$ | $1.04 \times 10^{-01}$ | $5.57 \times 10^{-03}$ | 0.219                     |
| 600            | $8.80 \times 10^{-02}$ | $4.08 \times 10^{-03}$ | $8.81 \times 10^{-02}$ | $4.08 \times 10^{-03}$ | 0.184                     |
| 700            | $7.47 \times 10^{-02}$ | $3.05 \times 10^{-03}$ | $7.49 \times 10^{-02}$ | $3.05 \times 10^{-03}$ | 0.156                     |
| 800            | $6.38 \times 10^{-02}$ | $2.30 \times 10^{-03}$ | $6.38 \times 10^{-02}$ | $2.30 \times 10^{-03}$ | 0.132                     |
| 900            | $5.48 \times 10^{-02}$ | $1.76 \times 10^{-03}$ | $5.47 \times 10^{-02}$ | $1.45 \times 10^{-03}$ | 0.113                     |
| 1000           | $4.72 \times 10^{-02}$ | $1.34 \times 10^{-03}$ | $4.68 \times 10^{-02}$ | $1.35 \times 10^{-03}$ | $9.66 \times 10^{-02}$    |

Table 2.10. The cross sections for  $t'$  signal at the process  $pp \rightarrow gb$  with  $P_T = 50$  GeV and cuts  $|\eta_{j,\gamma}| < -2.5$  at the center of mass energy 14 TeV for parametrization PII.

| $m_{t'}$ (GeV) | $ug \rightarrow g b$ | $cg \rightarrow gb$ | $gu \rightarrow g b$ | $gu \rightarrow g b$ | $\sigma_{Tot}(\text{pb})$ |
|----------------|----------------------|---------------------|----------------------|----------------------|---------------------------|
| 300            | 2.1                  | 0.994               | 2.16                 | 0.983                | 6.237                     |
| 400            | 1.56                 | 0.709               | 1.6                  | 0.705                | 4.574                     |
| 500            | 1.17                 | 0.504               | 1.17                 | 0.501                | 3.345                     |
| 600            | 0.891                | 0.368               | 0.894                | 0.355                | 2.51                      |
| 700            | 0.685                | 0.269               | 0.673                | 0.270                | 1.90                      |
| 800            | 0.510                | 0.199               | 0.510                | 0.199                | 1.42                      |
| 900            | 0.408                | 0.154               | 0.402                | 0.149                | 1.11                      |
| 1000           | 0.331                | 0.119               | 0.335                | 0.122                | 0.907                     |

Table 2.11. *The cross sections for  $t'$  signal at the process  $pp \rightarrow gb$  with  $P_T = 50$  GeV and cuts  $|\eta_{j,\gamma}| < -2.5$  at the center of mass energy 14 TeV for parametrization PIII*

| $m_{t'}$ (GeV) | $ug \rightarrow gb$ | $cg \rightarrow gb$ | $gu \rightarrow gb$ | $gu \rightarrow gb$ | $\sigma_{Tot}$ (pb) |
|----------------|---------------------|---------------------|---------------------|---------------------|---------------------|
| 300            | 17.6                | 8.14                | 17.5                | 8.12                | 51.4                |
| 400            | 12.2                | 5.34                | 12                  | 5.24                | 34.8                |
| 500            | 8.98                | 3.8                 | 8.65                | 3.76                | 25.19               |
| 600            | 6.96                | 2.85                | 6.92                | 2.67                | 19.4                |
| 700            | 5.91                | 1.97                | 5.31                | 2.04                | 15.23               |
| 800            | 4.53                | 1.63                | 4.54                | 1.65                | 12.35               |
| 900            | 3.91                | 1.36                | 3.96                | 1.36                | 10.59               |
| 1000           | 3.64                | 1.13                | 3.52                | 1.13                | 9.42                |

The signal cross sections depending on the  $t'$  masses for each channel in  $pp \rightarrow Zb$  process with cuts  $|\eta_{j,\gamma}| < -2.5$  and transverse momentum cuts  $P_T = 50$  GeV at the center of mass energy  $\sqrt{s} = 14$  TeV in table ( 2.12), table ( 2.13) and table ( 2.14 ) for PI, PII and PIII, respectively.

Table 2.12. *The cross sections for  $t'$  signal at the process  $pp \rightarrow Zb$  with  $P_T = 50$  GeV and cuts  $|\eta_{j,\gamma}| < -2.5$  at the center of mass energy 14 TeV for parametrization PI*

| $m_{t'}$ (GeV) | $ug \rightarrow Zb$    | $cg \rightarrow Zb$    | $gu \rightarrow Zb$    | $gu \rightarrow Zb$    | $\sigma_{Tot}$ (pb)    |
|----------------|------------------------|------------------------|------------------------|------------------------|------------------------|
| 300            | $2.59 \times 10^{-03}$ | $2.26 \times 10^{-04}$ | $2.59 \times 10^{-03}$ | $1.25 \times 10^{-04}$ | $5.53 \times 10^{-03}$ |
| 400            | $2.54 \times 10^{-03}$ | $1.03 \times 10^{-04}$ | $2.54 \times 10^{-03}$ | $1.03 \times 10^{-04}$ | $5.28 \times 10^{-03}$ |
| 500            | $2.41 \times 10^{-03}$ | $8.40 \times 10^{-05}$ | $2.41 \times 10^{-03}$ | $8.40 \times 10^{-05}$ | $4.99 \times 10^{-03}$ |
| 600            | $2.27 \times 10^{-03}$ | $6.89 \times 10^{-05}$ | $2.28 \times 10^{-03}$ | $6.89 \times 10^{-05}$ | $4.69 \times 10^{-03}$ |
| 700            | $2.13 \times 10^{-03}$ | $5.68 \times 10^{-05}$ | $2.13 \times 10^{-03}$ | $5.68 \times 10^{-05}$ | $4.37 \times 10^{-03}$ |
| 800            | $1.97 \times 10^{-03}$ | $4.69 \times 10^{-05}$ | $1.97 \times 10^{-03}$ | $4.69 \times 10^{-05}$ | $4.04 \times 10^{-03}$ |
| 900            | $1.82 \times 10^{-03}$ | $3.88 \times 10^{-05}$ | $1.82 \times 10^{-03}$ | $3.86 \times 10^{-05}$ | $3.72 \times 10^{-03}$ |
| 1000           | $1.65 \times 10^{-03}$ | $3.23 \times 10^{-05}$ | $1.63 \times 10^{-03}$ | $3.19 \times 10^{-05}$ | $3.34 \times 10^{-03}$ |

Table 2.13. *The cross sections for  $t'$  signal at the process  $pp \rightarrow Zb$  with  $P_T = 50$  GeV and cuts  $|\eta_{j,\gamma}| < -2.5$  at the center of mass energy 14 TeV for parametrization PII*

| $m_{t'}$ (GeV) | $ug \rightarrow Zb$    | $cg \rightarrow Zb$    | $gu \rightarrow Z b$   | $gu \rightarrow Zb$    | $\sigma_{Tot}$ (pb)    |
|----------------|------------------------|------------------------|------------------------|------------------------|------------------------|
| 300            | $2.71 \times 10^{-02}$ | $1.14 \times 10^{-02}$ | $2.72 \times 10^{-02}$ | $1.34 \times 10^{-02}$ | $7.91 \times 10^{-02}$ |
| 400            | $2.33 \times 10^{-02}$ | $9.50 \times 10^{-03}$ | $2.34 \times 10^{-02}$ | $9.56 \times 10^{-03}$ | $6.58 \times 10^{-02}$ |
| 500            | $1.96 \times 10^{-02}$ | $7.70 \times 10^{-03}$ | $1.97 \times 10^{-02}$ | $7.50 \times 10^{-03}$ | $5.45 \times 10^{-02}$ |
| 600            | $1.64 \times 10^{-02}$ | $6.17 \times 10^{-03}$ | $1.64 \times 10^{-02}$ | $6.14 \times 10^{-03}$ | $4.51 \times 10^{-02}$ |
| 700            | $1.40 \times 10^{-02}$ | $5.08 \times 10^{-03}$ | $1.42 \times 10^{-02}$ | $5.01 \times 10^{-03}$ | $3.83 \times 10^{-02}$ |
| 800            | $1.15 \times 10^{-02}$ | $4.05 \times 10^{-03}$ | $1.16 \times 10^{-02}$ | $4.06 \times 10^{-03}$ | $3.12 \times 10^{-02}$ |
| 900            | $9.96 \times 10^{-03}$ | $3.40 \times 10^{-03}$ | $9.93 \times 10^{-03}$ | $3.35 \times 10^{-03}$ | $2.66 \times 10^{-02}$ |
| 1000           | $8.62 \times 10^{-03}$ | $2.87 \times 10^{-03}$ | $8.58 \times 10^{-03}$ | $2.88 \times 10^{-03}$ | $2.30 \times 10^{-02}$ |

Table 2.14 *The cross sections for  $t'$  signal at the process  $pp \rightarrow Zb$  with  $P_T = 50$  GeV and cuts  $|\eta_{j,\gamma}| < -2.5$  at the center of mass energy 14 TeV for parametrization PII*

| $m_{t'}$ (GeV) | $ug \rightarrow Zb$ | $cg \rightarrow Zb$    | $gu \rightarrow Z b$ | $gu \rightarrow Zb$    | $\sigma_{Tot}$ (pb) |
|----------------|---------------------|------------------------|----------------------|------------------------|---------------------|
| 300            | 0.224               | $9.43 \times 10^{-02}$ | 0.223                | $9.47 \times 10^{-02}$ | 0.636               |
| 400            | 0.179               | $7.24 \times 10^{-02}$ | 0.183                | $7.18 \times 10^{-02}$ | 0.506               |
| 500            | 0.168               | $5.81 \times 10^{-02}$ | 0.170                | $5.78 \times 10^{-02}$ | 0.454               |
| 600            | 0.164               | $5.07 \times 10^{-02}$ | 0.132                | $4.92 \times 10^{-02}$ | 0.396               |
| 700            | 0.167               | $5.83 \times 10^{-02}$ | 0.130                | $4.44 \times 10^{-02}$ | 0.4                 |
| 800            | 0.123               | $4.19 \times 10^{-02}$ | 0.134                | $4.13 \times 10^{-02}$ | 0.340               |
| 900            | 0.128               | $3.72 \times 10^{-02}$ | 0.133                | $3.87 \times 10^{-02}$ | 0.337               |
| 1000           | 0.120               | $3.39 \times 10^{-02}$ | 0.126                | $3.36 \times 10^{-02}$ | 0.314               |

The cross sections for the backgrounds is given in table( 2.15) . We apply the following cuts,  $P_T = 50$  GeV and  $|\eta_{j,\gamma}| < -2.5$  at the center of mass energy  $\sqrt{S} = 14$  TeV to the process ( $pp \rightarrow \gamma b$ ), ( $pp \rightarrow gb$ ), ( $pp \rightarrow Zb$ ) for parametrization PI.

Table 2.15. *The cross sections for the backgrounds to the process*(pp  $\rightarrow$   $\gamma$ b ), ( pp  $\rightarrow$  gb), ( pp  $\rightarrow$  Zb) *with cuts*  $P_T=50$  GeV *and*  $|\eta_{j,\gamma}| < -2.5$  *at the center of mass energy* 14 TeV *for PI*

| $m_t(\text{GeV})$ | $\sigma_{\gamma b}(\text{pb})$ | $\sigma_{gb}(\text{pb})$ | $\sigma_{Zb}(\text{pb})$ | $\sigma_{\text{Tot}}(\text{pb})$ |
|-------------------|--------------------------------|--------------------------|--------------------------|----------------------------------|
| 300               | $1.41 \times 10^{-06}$         | $2.77 \times 10^{-04}$   | $1.17 \times 10^{-06}$   | $2.80 \times 10^{-04}$           |
| 400               | $1.39 \times 10^{-06}$         | $2.35 \times 10^{-04}$   | $1.33 \times 10^{-06}$   | $2.38 \times 10^{-04}$           |
| 500               | $1.31 \times 10^{-06}$         | $1.97 \times 10^{-04}$   | $1.35 \times 10^{-06}$   | $2.00 \times 10^{-04}$           |
| 600               | $1.15 \times 10^{-06}$         | $1.60 \times 10^{-04}$   | $1.27 \times 10^{-06}$   | $1.63 \times 10^{-04}$           |
| 700               | $9.98 \times 10^{-07}$         | $1.30 \times 10^{-04}$   | $1.15 \times 10^{-06}$   | $1.32 \times 10^{-04}$           |
| 800               | $8.56 \times 10^{-07}$         | $1.05 \times 10^{-04}$   | $1.01 \times 10^{-06}$   | $1.07 \times 10^{-04}$           |
| 900               | $7.27 \times 10^{-07}$         | $8.59 \times 10^{-05}$   | $8.85 \times 10^{-07}$   | $8.75 \times 10^{-05}$           |
| 1000              | $6.16 \times 10^{-07}$         | $7.00 \times 10^{-05}$   | $6.76 \times 10^{-07}$   | $7.13 \times 10^{-05}$           |

The cross sections for the backgrounds is given in table( 2.16) . We apply the following cuts,  $P_T = 50$  GeV and  $|\eta_{j,\gamma}| < -2.5$  at the center of mass energy  $\sqrt{S} = 14$  TeV to the process (pp  $\rightarrow$   $\gamma$ b ), ( pp  $\rightarrow$  gb), ( pp  $\rightarrow$  Zb) for parametrization PII.

Table 2.16. *The cross sections for the backgrounds to the process*(pp  $\rightarrow$   $\gamma$ b ), ( pp  $\rightarrow$  gb), ( pp  $\rightarrow$  Zb) *with cuts*  $P_T=50$  GeV *and*  $|\eta_{j,\gamma}| < -2.5$  *at the center of mass energy* 14 TeV *for PII*

| $m_t(\text{GeV})$ | $\sigma_{\gamma b}(\text{pb})$ | $\sigma_{gb}(\text{pb})$ | $\sigma_{Zb}(\text{pb})$ | $\sigma_{\text{Tot}}(\text{pb})$ |
|-------------------|--------------------------------|--------------------------|--------------------------|----------------------------------|
| 300               | $1.46 \times 10^{-06}$         | $2.84 \times 10^{-04}$   | $1.22 \times 10^{-06}$   | $2.86 \times 10^{-04}$           |
| 400               | $1.52 \times 10^{-06}$         | $2.54 \times 10^{-04}$   | $1.44 \times 10^{-06}$   | $2.57 \times 10^{-04}$           |
| 500               | $1.43 \times 10^{-06}$         | $2.20 \times 10^{-04}$   | $1.48 \times 10^{-06}$   | $2.23 \times 10^{-04}$           |
| 600               | $1.29 \times 10^{-06}$         | $1.78 \times 10^{-04}$   | $1.42 \times 10^{-06}$   | $1.80 \times 10^{-04}$           |
| 700               | $1.11 \times 10^{-06}$         | $1.45 \times 10^{-04}$   | $1.29 \times 10^{-06}$   | $1.47 \times 10^{-04}$           |
| 800               | $9.98 \times 10^{-07}$         | $1.23 \times 10^{-04}$   | $1.17 \times 10^{-06}$   | $1.25 \times 10^{-04}$           |
| 900               | $8.27 \times 10^{-07}$         | $9.96 \times 10^{-05}$   | $1.01 \times 10^{-06}$   | $1.01 \times 10^{-04}$           |
| 1000              | $6.97 \times 10^{-07}$         | $8.01 \times 10^{-05}$   | $8.71 \times 10^{-07}$   | $8.16 \times 10^{-05}$           |

The cross sections for the backgrounds is given in table ( 2.17). We apply the following cuts  $P_T = 50$  GeV and  $|\eta_{j,\gamma}| < -2.5$  at the center of mass energy  $\sqrt{s} = 14$  TeV to the process  $(pp \rightarrow \gamma b)$ ,  $(pp \rightarrow gb)$ ,  $(pp \rightarrow Zb)$  is given in table( 2.17) for parametrization PIII.

Table 2.17. *The cross sections for the backgrounds to the process  $(pp \rightarrow \gamma b)$ ,  $(pp \rightarrow gb)$ ,  $(pp \rightarrow Zb)$  with cuts  $P_T=50$  GeV and  $|\eta_{j,\gamma}| < -2.5$  at the center of mass energy 14 TeV for PIII*

| $m_t$ (GeV) | $\sigma_{\gamma b}(\text{pb})$ | $\sigma_{gb}(\text{pb})$ | $\sigma_{Zb}(\text{pb})$ | $\sigma_{\text{Tot}}(\text{pb})$ |
|-------------|--------------------------------|--------------------------|--------------------------|----------------------------------|
| 300         | $4.46 \times 10^{-06}$         | $8.71 \times 10^{-04}$   | $3.74 \times 10^{-06}$   | $8.79 \times 10^{-04}$           |
| 400         | $5.08 \times 10^{-06}$         | $8.40 \times 10^{-04}$   | $4.84 \times 10^{-06}$   | $8.50 \times 10^{-04}$           |
| 500         | $4.93 \times 10^{-06}$         | $7.51 \times 10^{-04}$   | $5.11 \times 10^{-06}$   | $7.61 \times 10^{-04}$           |
| 600         | $4.46 \times 10^{-06}$         | $6.24 \times 10^{-04}$   | $4.96 \times 10^{-06}$   | $6.33 \times 10^{-04}$           |
| 700         | $4.05 \times 10^{-06}$         | $5.24 \times 10^{-04}$   | $4.61 \times 10^{-06}$   | $5.33 \times 10^{-04}$           |
| 800         | $3.43 \times 10^{-06}$         | $4.23 \times 10^{-04}$   | $4.03 \times 10^{-06}$   | $4.31 \times 10^{-04}$           |
| 900         | $2.98 \times 10^{-06}$         | $3.55 \times 10^{-04}$   | $3.62 \times 10^{-06}$   | $3.61 \times 10^{-04}$           |
| 1000        | $2.54 \times 10^{-06}$         | $2.92 \times 10^{-04}$   | $3.19 \times 10^{-06}$   | $2.98 \times 10^{-04}$           |

According to results in preceding tables for the cross sections to the processes at center of mass energy  $\sqrt{s} = 14$  GeV with cuts  $|\eta_{j,\gamma}| < -2.5$  and transverse momentum cuts  $P_T=50$  GeV, we can observe that, the cross section decreases as the mass increases for PI, PII and PIII.

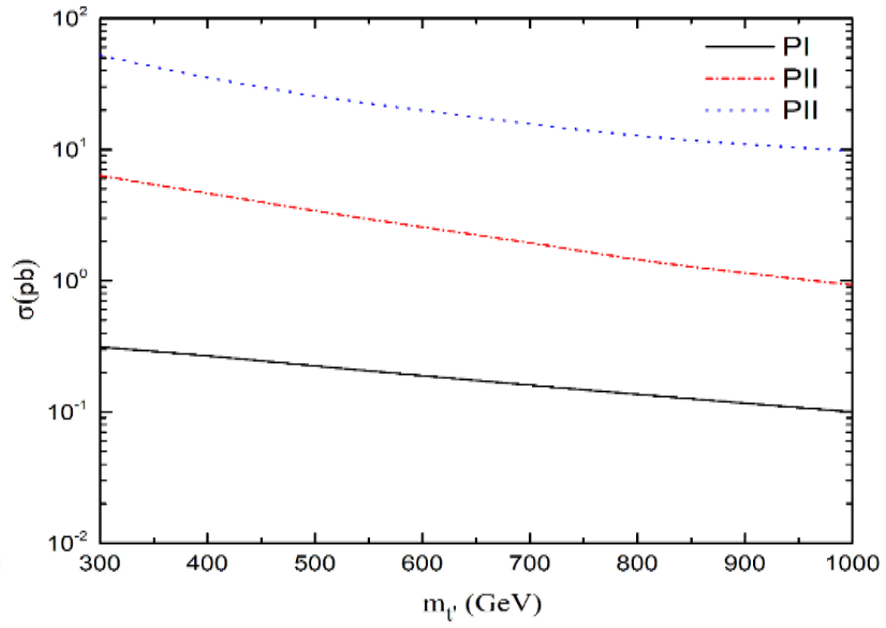


Figure 2.2. Total cross sections for the signal with cuts  $P_T=50$  GeV and  $|\eta_{j,\gamma}| < -2.5$  at the center of mass energy  $\sqrt{S} = 14$  TeV for PI, PII and PIII.

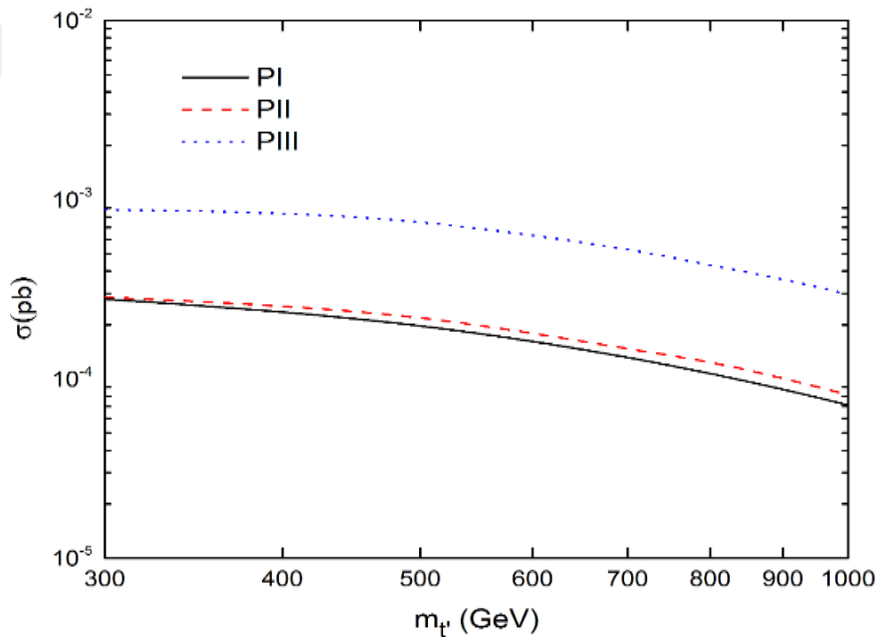


Figure 2.3. Total cross sections for the backgrounds with cuts  $P_T=50$  GeV and  $|\eta_{j,\gamma}| < -2.5$  at the center of mass energy  $\sqrt{S} = 14$  TeV for PI, PII and PIII

As we can see in the Figures ( 2.2 ) and (2.3), we can conclude that the production cross section decreases as the mass increases for PI PII and PIII.

As the last step in our work in this thesis, we used statistical significance in order to find the limits of discovery,

$$SS = \sqrt{2 \left[ (S + B) \ln \left( 1 + \frac{S}{B} \right) - S \right]} \quad (2.8)$$

Where, B is the number of background events and S is the number of signal events.

In table (2.18) the statistical significances of signal and the backgrounds cross sections with cuts  $P_T=50$  GeV and  $|\eta_{j,\gamma}| < 2.5$  for PI, PII and PIII.

Table 2.18. The statistical significances values for backgrounds and signal cross sections of  $t'$  for PI, PII and PIII).

| $m_{t'}$ | Statistical Significance |            |             |
|----------|--------------------------|------------|-------------|
|          | SS ( PI )                | SS ( PII ) | SS ( PIII ) |
| 300      | 613                      | 3379       | 10214       |
| 400      | 567                      | 2861       | 8260        |
| 500      | 520                      | 2427       | 6961        |
| 600      | 479                      | 2094       | 6102        |
| 700      | 442                      | 1815       | 5401        |
| 800      | 411                      | 1557       | 4858        |
| 900      | 381                      | 1378       | 4529        |
| 1000     | 354                      | 1249       | 4293        |

### 3. CONCLUSION

This thesis discusses the possibility of producing and decay for new heavy quark  $t'$  through anomalous interactions at LHC with the center of mass energy  $\sqrt{s} = 14$  TeV. First, the decay widths and the branching rates of quark  $t'$  depend on anomalous coupling  $\kappa/\Lambda$  at the same mass. Secondly, we calculated signal and the backgrounds cross sections for process  $pp \rightarrow W^+ bV^+ X$  to find the limits of discovery with PI, PII and PIII.

As a result of all the above and looking at the statistical significance we find that the new heavy  $t'$  quark at LHC can be observed through the anomalous vertices.



## REFERENCES

- Aad, G., Abajyan, T., Abbott, B., Abdallah, J., Khalek, S. A., Abdelalim, A. A., AbouZeid, O. S. vd. (2012). Search for a Heavy Top-Quark Partner in Final States with Two Leptons with the ATLAS Detector at the LHC. *Journal of High Energy Physics*, (11).
- Aad, G., Abbott, B., Abdallah, J., Abdelalim, A. A., Abdesselam, A., Abdinov, O., ... Abreu, H. vd. (2012). Search for Down-Type Fourth Generation Quarks with the ATLAS detector in events with one lepton and hadronically decaying W bosons. *Physical Review Letters*, 109 (3), 032001.
- Aad, G., Abbott, B., Abdallah, J., Khalek, S. A., Abdelalim, A. A., Abdesselam, A., Abramowicz, H. vd. (2012). Search for Heavy Vector-Like Quarks Coupling to Light Quarks in Proton-Proton Collisions at  $s = 7$  TeV with the ATLAS detector. *Physics Letters B*, 712 (1-2), 22-39.
- Aad, G., Abbott, B., Abdallah, J., Khalek, S. A., Abdinov, O., Aben, R., Abreu, H. vd. (2014). Search for Pair and Single Production of New Heavy Quarks that Decay to a Z Boson and a Third-Generation Quark in pp Collisions at  $s = 8$  TeV with the ATLAS Detector. *Journal of High Energy Physics*, (11), 104.
- Altarelli, G. (2005). The Standard Model of Particle Physics. arXiv Preprint hep-ph/0510281. *CERN-PH-TH*, 206.
- Aurenche, P. (1997). The Standard Model of Particle Physics. *Symmetries in Physics*, 169.
- Çakır, İ. T., Kuday, S., & Çakır, O. (2015). Production and Decay of Up-Type and Down-Type New Heavy Quarks Through Anomalous Interactions at the LHC. *Advances in High Energy Physics*.
- Dainese, A., Wiedemann, U. A., Armesto, N., d'Enterria, D., Jowett, J. M., Lansberg, J. P., Albacete, J. L. vd. (2016). Heavy ions at the Future Circular Collider. *arXiv Preprint arXiv:1605.01389*.
- Franzini, P. (2002). "*Elementary Particle Physics Lecture Notes Spring 2002*."
- Gasiorowicz, S. (1966). *Elementary Particle Physics* (pp. 436-9). New York: Wiley.
- Griffiths, D. (2008). *Introduction to Elementary Particles*. John Wiley & Sons.
- Kane, G. L. (1993). Modern Elementary Particle Physics: the Fundamental Particles and Forces. *Addison-Wesley*.
- Kibble, T. W. (2015). The Standard Model of Particle Physics. *European Review*, 23 (1), 36-44.

- Lapsien, T. (2016). *Studies of top Tagging Identification Methods and Development of a New Heavy Object Tagger* (Doctoral dissertation, Deutsches Elektronen-Synchrotron, DESY).
- Mandrysch, R. (2013). *Search for Fourth Generation Down-Type Quarks in the Same-Sign Dilepton Channel with ATLAS at a Centre-of-Mass-Energy,  $\sqrt{s}=7$  TeV*. Berlin.
- Mann, R. (2011). *An Introduction to Particle Physics and the Standard Model*. CRC press.
- Patrignani, C., & Particle Data Group. (2016). Review of Particle Physics. *Chinese physics C*, 40 (10), 100001.
- Perkins, D. H. (2000). *Introduction to High Energy Physics*. Cambridge University Press.
- Pukhov, A., Boos, E., Dubinin, M., Edneral, V., Ilyin, V., Kovalenko, D., Semenov, A. vd. (1999). CompHEP-a Package for Evaluation of Feynman Diagrams and Integration over Multi-Particle Phase Space. *User's Manual for Version 33*. arXiv preprint hep-ph/9908288.
- Ragheb, M. (?) "Constitution of Matter, The Standard Model."
- Renton, P., & Interactions, E. (1990). *An Introduction to the Physics of Quarks and Leptons*. Cambridge university.
- Senol, A., Tasci, A. T., & Ustabas, F. (2011). Anomalous Single Production of Fourth Generation  $t'$  Quarks at ILC and CLIC. *Nuclear Physics B*, 851 (2), 289-297.
- Serkin, L. (2016). *Search for the Standard Model Higgs Boson Produced in Association with a pair of top Quarks and Decaying into a  $b\bar{b}$  pair in the Single Lepton Channel at  $\sqrt{s}=8$  TeV with the ATLAS Experiment at the LHC*. ICTP, Trieste.
- Stoyle, R. J. B. (1997). *EUREKA. Physics of Particles, Matter and the Universe: Institute of Physics Publishing, Bristol Philadelphia, USA*.
- URL-1 <http://cronodon.com/Atomic/QCD.html> It has taken on 15/10/2017 .
- URL-2 [https://www.nsf.gov/news/mmg/mmg\\_disp.jsp?med\\_id=75529&from](https://www.nsf.gov/news/mmg/mmg_disp.jsp?med_id=75529&from) It has taken on 24/10/2017 .
- URL-3 [http://www.easyparticles.com/p/large-hadron-collider\\_18.html](http://www.easyparticles.com/p/large-hadron-collider_18.html) It has taken on 5/11/2017.
- URL-4 <https://www.wsws.org/en/articles/2013/03/23/higg-m23.html> It has taken on 5/11/2027.

- URL-5 <https://sciencenode.org/spotlight/improving-data-analytics-better-science.php>  
It has taken on 13/11/2017.
- URL-6 <http://bigthink.com/paul-ratner/weasel-shuts-down-large-hadron-collider> It  
has taken on 18/11/2017.
- URL-5 <http://sciexplorer.blogspot.com.tr/2011/01/our-universe-part-9-lepton-epoch.html> It has taken on 25/11/2017.
- URL-8 <https://www.slideshare.net/seenet/to-the-standard-model-ion-cotaescu> It has  
taken on 25/11/2017.
- URL-9 [https://home.fnal.gov/~cheung/rtes/RTESWeb/LQCD\\_site/pages/weakforce.htm](https://home.fnal.gov/~cheung/rtes/RTESWeb/LQCD_site/pages/weakforce.htm)  
It has taken on 29/11/2017.
- URL-10 <http://physicsnet.co.uk/a-level-physics-as-a2/particles-radiation/particles-antiparticles-photons/> It has taken on 30/11/2017.
- URL-11 <http://inspirehep.net/record/1297394/plots> It has taken on 4/12/2017.
- URL-12 <http://www.hep.phy.cam.ac.uk/atlas/> It has taken on 15/12/2017.
- URL-13 <https://df.units.it/en/research/researchareas/researchgroups/5368> It has taken  
on 15/12/2017.
- URL-14 [http://alicematters.web.cern.ch/?q=tiziano\\_virgili](http://alicematters.web.cern.ch/?q=tiziano_virgili) It has taken on 21/12/2017.

## CV

Name, Surname : Mouna Mansur Ali ABUKRHIS  
Date and Birth of Place : Libya- Tripoli / 1985  
Social Status : Married  
The Foreign Language : English  
E-mail : najimaali81@gmail.com



### **Education Background**

High School : Basic Sciences  
Bachelor's Degree : Physics, Faculty of Education.  
Post Graduate : Kastamonu University, Department of Physics

### **Professional Experience**

Workplace : Faculty of Education - Tripoli University - Tripoli - Libya (2012-2014)